Exon, N.F., Kennett, J.P., and Malone, M.J. (Eds.)
Proceedings of the Ocean Drilling Program, Scientific Results Volume 189

7. Data Report: Miocene Calcareous Nannofossil Biostratigraphy, ODP Leg 189, Tasmanian Seaway[1]

Kristeen L. McGonigal,[2, 3] and Wuchang Wei[4]

F1. Location map, p. 15.

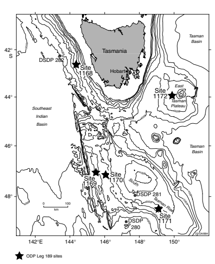

INTRODUCTION

During Ocean Drilling Program (ODP) Leg 189, five sites were drilled in the Tasmanian Seaway with the objective to constrain the paleoceanographic implications of the separation of Australia from Antarctica and to elucidate the paleoceanographic developments throughout the Neogene (Shipboard Scientific Party, 2001a). Sediments ranged from Cretaceous to Quaternary in age and provided the opportunity to describe the paleoenvironments in the Tasman Seaway prior to, during, and after the separation of Australia and Antarctica. This study will focus on postseparation distribution of calcareous nannofossils through the Miocene. Miocene sediments were recovered at all five Leg 189 sites (Fig. **F1**), and four of these sites were studied in detail to determine the calcareous nannofossil biostratigraphy.

Hole 1168A, located on the western Tasmanian margin, contains a fairly continuous Miocene record and could be easily zoned using the Okada and Bukry (1980) zonation. Analysis of sediments from Hole 1169A, located on the western South Tasman Rise, was not included in this study, as the recovered sediments were highly disturbed and unsuitable for further analysis (Shipboard Scientific Party, 2001c). Holes 1170A, 1171A, and 1171C are located on the South Tasman Rise south of the modern Subtropical Front (STF). They revealed incomplete Miocene sequences intersected by an early Miocene and late Miocene hiatus and could only be roughly zoned using the Okada and Bukry zonation. Similarly, Hole 1172A, located on the East Tasman Plateau, contains a Miocene sequence with a hiatus in the early Miocene and in the late Miocene and could only be roughly zoned using the Okada and

[1]McGonigal, K.L., and Wei, W., 2003. Data report: Miocene calcareous nannofossil biostratigraphy, ODP Leg 189, Tasmanian Seaway. *In* Exon, N.F., Kennett, J.P., and Malone, M.J. (Eds.), *Proc. ODP, Sci. Results,* 189, 1–39 [Online]. Available from World Wide Web: <http://www-odp.tamu.edu/publications/189_SR/VOLUME/CHAPTERS/110.PDF>. [Cited YYYY-MM-DD]
[2]Department of Geological Sciences, Florida State University, Tallahassee FL 32306, USA. **roessig@gly.fsu.edu**
[3]Sonnenbrunnenstrasse 16, 79112 Freiburg-Waltershofen, Germany.
[4]PaleoServe, 4389 Corte De La Fonda, San Diego CA 92130, USA.

Initial receipt: 20 January 2003
Acceptance: 16 May 2003
Web publication: 10 October 2003
Ms 189SR-110

Bukry (1980) zonation. This study aims to improve calcareous nannofossil biostratigraphic resolution in this sector of the mid to high southern latitudes. This paper will present abundance, preservation, and stratigraphic distribution of calcareous nannofossils through the Miocene and focus mainly on biozonal assignment.

MATERIALS AND METHODS

Samples were prepared using standard nannofossil smear slide techniques. Unprocessed sediment was smeared on a glass coverslip, dried, and then mounted on a glass slide using Norland optical adhesive mounting media. The nannofossil biostratigraphy presented here is based on examination of one to two samples per section using a Zeiss Axioscope under 625×–1560× magnification, employing phase-contrast, differential-interference contrast, and cross-polarized light. Core catcher samples were not examined for this study, but shipboard data from these samples were included to determine the depth of some biostratigraphic events. Semiquantitative abundance of each nannofossil species was recorded based on at least 300 nannofossils randomly encountered on the smear slide. Relative overall abundance of nannofossils in the samples is represented by the following abbreviations:

V = very abundant (>100 specimens per 10 fields of view [FOV]).
A = abundant (11–100 specimens per 10 FOV).
C = common (6–10 specimens per 10 FOV).
F = few (1–5 specimens per 10 FOV).
R = rare (1 specimen per >10 FOV).

Preservation of the calcareous nannofossil assemblage was determined as follows:

G = good (individual specimens exhibit little or no dissolution or overgrowth; diagnostic characteristics are preserved and nearly all of the specimens can be identified).
M = moderate (individual specimens show evidence of dissolution or overgrowth; some specimens cannot be identified to the species level).
P = poor (individual specimens exhibit considerable dissolution or overgrowth; many specimens cannot be identified to the species level).

Range charts presented herein as Tables **T1, T2, T3, T4,** and **T5.** were created with BugWin software (Bugware, Inc.) using these measurements. Calcareous nannofossil species considered in this paper are listed in the **"Appendix,"** p. 13, where they are arranged alphabetically by generic epithet. Additional notes clarifying species concepts are also included in the **"Appendix,"** p. 13. Key marker species were photographed for taxonomic clarity (Plate **P1**). Bibliographic references for these taxa can be found in Perch-Nielsen (1985) and Bown (1998).

ZONATION

The standard zonal scheme of Okada and Bukry (1980), with some additional bioevents, was applied to Leg 189 Miocene sediments (Fig.

T1. Miocene calcareous nannofossils, Hole 1168A, p. 17.

T2. Oligocene/Miocene calcareous nannofossils, Hole 1168A, p. 18.

T3. Miocene calcareous nannofossils, Hole 1170A, p. 19.

T4. Miocene calcareous nannofossils, Holes 1171A and 1171C, p. 20.

T5. Miocene calcareous nannofossils, Hole 1172A, p. 21.

P1. *Discoaster,* p. 24.

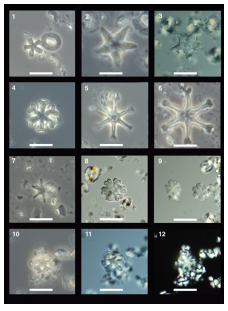

F2). Several low-latitude species used as zonal markers by Okada and Bukry (1980) are rare to absent in Leg 189 sediments, which forced the combination of several zones. Additional Miocene biostratigraphic events have been recognized by many workers (Raffi et al., 1995, 1998; deKaenel and Villa, 1996; Backman and Raffi, 1997; Maiorano and Monechi, 1998), and some of these events were included to improve biostratigraphic resolution and estimate zonal boundaries where marker species were absent.

BIOSTRATIGRAPHIC RESULTS

Hole 1168A

Hole 1168A (42°36′S, 144°24′E) was drilled in 2463 m water depth on the western continental slope of Tasmania. Miocene sediments were recognized between Samples 189-1168A-10H-2, 15 cm, and 47X-4, 68 cm, and the stratigraphic distribution of nannofossils is given in Table T1. An expanded Oligocene/Miocene (O/M) boundary section was recovered at Site 1168, and high-resolution biostratigraphic results across this interval are included in Table T2. Key biohorizons are listed in Table T6, along with their sample interval and average depth. The Miocene sediments consist of nannofossil ooze, foraminifer-bearing nannofossil chalk, clay-bearing nannofossil chalk, and nannofossil claystone (Shipboard Scientific Party, 2001b). Calcareous nannofossils are abundant and moderately preserved in all samples.

The Miocene/Pliocene boundary (CN9b/CN10) is placed between Samples 189-1168A-10H-1, 15 cm, and 10H-2, 16 cm, based on the last occurrence (LO) of *Triquetrorhabdulus rugosus* (5.23 Ma). *Discoaster quinqueramus* (5.53 Ma), whose LO was used by Okada and Bukry (1980) to mark this boundary, is not recorded in Hole 1168A. The interval from 189-1168A-10H-2, 16 cm, to 12H-6, 15 cm, represents the late Miocene *Amaurolithus primus* CN9b Subzone of Okada and Bukry (1980), based on the first occurrence (FO) of *A. primus*. Characteristic nannofossils of this zone are *A. primus, Amaurolithus delicatus, Calcidiscus leptoporus, Reticulofenestra minuta, Reticulofenestra minutula,* and *Reticulofenestra producta*. The FO of *A. delicatus* and the top of the *Reticulofenestra pseudoumbilicus* >7 µm paracme also occur in this interval.

Several of the late and middle Miocene zones had to be combined, as they are subdivided on the presence of certain discoaster species which are rare to absent in Hole 1168A. *Discoaster loeblichii* and *Discoaster surculus* were not consistently present in Hole 1168A, whereas *Discoaster berggrenii* and *Discoaster neorectus* were not recorded. Therefore, the *D. berggrenii* Subzone CN9a and the *D. neorectus* Subzone CN8b were combined, and the bottom of the *R. pseudoumbilicus* paracme >7 µm is used to approximate the base of this combined zone. According to Young (1998), this event is slightly older than the FO of *D. neorectus* and *D. loeblichii*. The combined zone extends down to Sample 189-1168A-15X-2, 15 cm, and is characterized by the low abundance of *R. pseudoumbilicus* >7 µm and abundant *C. leptoporus, Coccolithus pelagicus, R. minuta, R. minutula,* and *Reticulofenestra perplexa*. The closely spaced FO of *Sphenolithus abies,* the LO of *Minylitha convallis,* and a sharp increase in the abundance of *R. producta* may indicate a condensed section at ~129 meters below seafloor (mbsf). Above this depth, discoaster diversity increases and an influx of diatom microfossils was noted.

F2. Nannofossil zones and datums, p. 16.

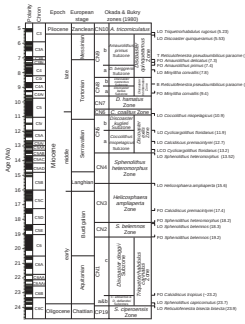

T6. Key Miocene biohorizons, p. 22.

The base of the *Discoaster bellus* CN8a Subzone was approximated by the FO of *M. convallis,* as *Discoaster hamatus* was not recorded in Hole 1168A. Subzone CN8a extends down to Sample 189-1168A-17X-4, 15 cm (152.70 mbsf). *Catinaster calyculus* was not recorded in Hole 1168A, and only one specimen of *Catinaster coalitus* was noted, causing the combination of the *D. hamatus* CN7 Zone and the *C. coalitus* CN6 Zone. The LO of *Coccolithus miopelagicus* is used to approximate the base of Zone CN6 in the absence of *C. coalitus* (Raffi and Flores, 1995). This interval extends down to Sample 189-1168A-20X-5, 15 cm (183.0 mbsf), and is characterized by common *C. leptoporus, C. pelagicus, Reticulofenestra gelida, R. minutula,* and *R. perplexa*.

The base of the CN5b *Discoaster kugleri* Subzone was recognized by the LO of *Cyclicargolithus floridanus* and is placed between Sample 189-1168A-22X-2, 15 cm, and 22X-3, 15 cm (197.8 mbsf). This interval is characterized by *C. leptoporus, Calcidiscus macintyrei, C. pelagicus, R. pseudoumbilicus, R. gelida, R. minuta, R. minutula,* and by few *Calcidiscus tropicus* and *Sphenolithus compactus*.

The LO of *Sphenolithus heteromorphus* is placed between Sample 189-1168A-26X-7, 15 cm, and 26X-7, 15 cm (242.2 mbsf), marking the base of the *C. miopelagicus* CN5a Subzone. The assemblage includes abundant *C. leptoporus, C. macintyrei, C. pelagicus, R. pseudoumbilicus, R. gelida, R. minuta,* and *R. minutula*. *C. tropicus, Discoaster* spp. 6-rayed, *Geminilithella rotula, Helicosphaera paleocarteri, Pyrocyclus hermosus, Reticulofenestra haqii, S. compactus,* and *Sphenolithus moriformis* are commonly present. The LO of *Calcidiscus premacintyrei* (221.5 mbsf) and the last common occurrence (LCO) of *C. floridanus* (236.2 mbsf) occur within Subzone CN5a.

The *S. heteromorphus* CN4 and the *Helicosphaera ampliaperta* CN3 Zones were combined, as *H. ampliaperta* was present in only two samples in Hole 1168A. The base of the combined zone is marked by the FO of *S. heteromorphus* at 293.8 mbsf (Samples 189-1168A-32X-2, 15 cm, through 32X-3, 15 cm). This interval contains abundant *C. pelagicus, C. floridanus, R. haqii,* and *R. minuta*. Common species are *C. leptoporus, C. macintyrei, C. premacintyrei, Cyclicargolithus abisectus, Discoaster* spp. 6-rayed, *G. rotula, H. paleocarteri, Pyrocyclus orangensis, S. compactus,* and *S. moriformis*. The LO of *Sphenolithus belemnos,* which is used in the Martini (1971) zonal scheme to mark the base of his *H. ampliaperta* NN4 Zone (roughly equivalent to Okada and Bukry's CN3 Zone), occurs at 299.6 mbsf, slightly below the FO of *S. heteromorphus*.

The FO of *S. belemnos* marks the base of the *S. belemnos* CN2 Zone and occurs between Samples 189-1168A-34X-3, 15 cm, and 34X-4, 15 cm (313.9 mbsf). Abundant *C. pelagicus, C. floridanus, R. minuta,* and *R. minutula* were recorded in this interval.

The ~5-m.y.-long *Triquetrorhabdulus carinatus* CN1 Zone is subdivided into three subzones by Okada and Bukry (1980), based on the FO of *Discoaster druggii* (CN1a/CN1b) and the acme event of *C. abisectus* (CN1b/CN1c). *D. druggii* was not recorded in any Leg 189 sediments, and the acme event of *C. abisectus* is poorly described and difficult to quantitatively determine (Young, 1998). Recent work has refined the biostratigraphy of this interval with several additional bioevents (Olafsson, 1989; deKaenel and Villa, 1996; Maiorano and Monechi, 1998). Unfortunately, much of this work has described tropical to subtropical species, which were not consistently recorded in Leg 189 sediments or could not be identified because of moderate preservation. The FO of *C. tropicus* <6 µm was listed by deKaenel and Villa (1996) as occurring just above the Zone NN1/NN2 (Martini, 1971) boundary (approximate to

the Subzone CN1b/CN1c boundary). The FO of *C. tropicus* is used here to estimate the Subzone CN1b/CN1c boundary and occurs between Samples 189-1168A-43X-5, 2 cm, and 43X-5, 40 cm (402.71 mbsf). The CN1c Subzone contains common *C. pelagicus, C. floridanus, Discoaster* spp. 6-rayed, *R. haqii, R. minuta,* and *R. minutula.*

The base of the CN1b *Discoaster deflandrei* Subzone is approximated here by the LO of *Sphenolithus capricornutus* at 437.39 mbsf (Samples 189-1168A-47X-2, 78 cm, to 47X-2, 120 cm). This interval is similar to the CN1c Subzone except for the absence of *C. tropicus* and the increased abundance of *Helicosphaera bramlettei* and *Helicosphaera compacta*. The Oligocene/Miocene boundary (CN1a/CP19) is placed at 439.94 mbsf between Samples 189-1168A-47X-4, 40 cm, and 47X-4, 68 cm, based on the LO of *Reticulofenestra bisecta bisecta.*

Hole 1170A

Hole 1170A (47°09′S, 146°02′E) was drilled in 2704 m water depth on the South Tasman Rise (Fig. **F1**), south of the modern STF. Miocene sediments were recognized between Samples 189-1170A-15H-4, 60 cm, and 42X-3, 110 cm, and the stratigraphic distribution of nannofossils is given in Table **T3.** Key biohorizons are listed in Table **T6,** along with their sample interval and average depth. The Miocene sediments consist of nannofossil ooze, foraminifer-bearing nannofossil chalk, nannofossil chalk, and nannofossil claystone (Shipboard Scientific Party, 2001d). Calcareous nannofossils were abundant and moderately preserved in all samples.

The Miocene/Pliocene boundary (CN9b/CN10) is placed between Samples 189-1170-15H-3, 60 cm, and 15H-4, 60 cm (129.32 mbsf), based on the LO of *T. rugosus*. The late Miocene *A. primus* CN9b Subzone, based on the FO of *A. primus,* contains abundant *C. leptoporus, C. pelagicus, R. gelida, R. minutula,* and *R. perplexa.*

Coring disturbance in some sections of this interval was quite extreme (Shipboard Scientific Party, 2001d), and core sections that were disturbed (based on visual examination of core photos) were excluded from this report. The FO of *A. primus, A. delicatus,* and the top of the *R. pseudoumbilicus* >7 µm paracme occur between the bottom of Core 17H and the top of Core 19X. Coring disturbance was extreme in Core 18H, the last advanced piston corer (APC) core taken in Hole 1170A, and the entire core was unsuitable for analysis. This complicated the determination of the base of the *A. primus* Subzone, which is tentatively placed between Samples 189-1170A-17H-CC and 19X-1, 60 cm. A possible hiatus exists across this boundary, but the core disturbance complicates interpretation of such an event (for further discussion, see **Stickley et al.,** this volume).

The Okada and Bukry (1980) *D. berggrenii* CN9a Subzone and the *D. neorectus* CN8b Subzone were combined, as at Site 1168, and the base of Subzone CN8b is approximated by the bottom of the *R. pseudoumbilicus* >7 µm paracme event. This event occurs between Samples 189-1170A-21X-2, 60 cm, and 21X-3, 60 cm, at 179.15 mbsf. This interval is characterized by the low abundance of *R. pseudoumbilicus* >7 µm and the presence of *C. leptoporus, C. pelagicus, R. minuta, R. minutula,* and *R. perplexa.* Low numbers of *C. macintyrei, Discoaster* spp. 6-rayed, *S. moriformis* <6 µm, and *T. rugosus* were recorded in this interval.

The lack of marker species forced the combination of several late Miocene zones. The next discernible marker event is the LO of *C. miopelagicus,* used here to mark the base of the *C. coalitus* CN6 Zone between

Samples 189-1170A-25X-2, 60 cm, and 25X-3, 60 cm (217.55 mbsf). Common *C. leptoporus, C. pelagicus, R. gelida, R. minutula,* and *R. perplexa* are present throughout this interval. Discoasters are less abundant in this interval than in the overlying sediments.

The LO of *C. floridanus* marks the base of the *D. kugleri* CN5b Subzone between Samples 189-1170A-28X-4, 60 cm, and 28X-5, 60 cm (249.35 mbsf). This interval contains abundant *C. pelagicus, R. gelida, R. minutula,* and *R. perplexa*. The FO of *R. perplexa* is coincident with the base of this subzone. Discoasters are absent throughout this interval.

Sphenolithus heteromorphus was not recorded in situ in Hole 1170A; therefore, the top of the *S. heteromorphus* CN4 Zone (13.52 Ma) is approximated by the LCO of *C. floridanus* (13.2 Ma). The CN4/CN5a boundary is placed between Samples 189-1170A-31X-4, 60 cm, and 31X-5, 60 cm (278.15 mbsf). *Calcidiscus leptoporus, C. pelagicus, R. gelida,* and *R. minutula* are abundant in this interval.

The lack of consistently present *H. ampliaperta* forced the combination of Zones CN4 and CN3, as at Site 1168. The FO of *C. premacintyrei* (17.4 Ma) between Samples 189-1170A-35X-2, 60 cm, and 35X-3, 60 cm (312.95 mbsf), is used to roughly approximate the base of the *H. ampliaperta* CN3 Zone, as *S. heteromorphus* (FO = 18.2 Ma) and *S. belemnos* (FO = 18.3 Ma) were not recorded in situ in Hole 1170A. The FO of *C. premacintyrei* is easily detected, and this bioevent has the potential to be a key marker in mid- to high-latitude areas where sphenoliths are generally absent. This interval contains abundant *C. pelagicus, C. floridanus,* and *R. minutula*. Common species are *C. leptoporus, C. premacintyrei, C. tropicus, Discoaster* spp. 6-rayed, *G. rotula, H. paleocarteri,* and *R. gelida*.

The base of the *S. belemnos* CN2 Zone could not be identified in Hole 1170A. The FO of *C. tropicus* between Samples 189-1170A-41X-5, 60 cm, and 41X-6, 60 cm, places the base of the CN1c Subzone at 375.9 mbsf. The combined CN1a/CN1b Subzone continues down to 382.25 mbsf (Samples 189-1170A-42X-3, 110 cm, through 42X-4, 60 cm), where the LO of *R. bisecta bisecta* occurs. Within the CN1a/CN1b Subzone the simultaneous LOs of *Clausicoccus obrutus, Hughesius tasmaniae,* and *Reticulofenestra stavensis* were noted at ~380 mbsf, indicating a hiatus/condensed interval just above the O/M boundary. Magnetostratigraphic (**Stickley et al.,** this volume) and benthic oxygen isotope (**Pfuhl and McCave,** this volume) work suggest continuous though condensed sedimentation across the O/M boundary.

Holes 1171A and 1171C

Hole 1171A (48°30′S, 149°07′E) was drilled in 2148 m water depth on the South Tasman Rise (Fig. **F1**) in subantarctic waters. Hole 1171A was cored to 124.4 mbsf and bottomed in upper Miocene sediments (Shipboard Scientific Party, 2001e). To construct a complete Miocene section, samples were also taken from Hole 1171C (48°30′S, 149°07′E; 2148 m water depth) beginning at 110 mbsf. Miocene sediments were recognized between Samples 189-1171A-7H-1, 15 cm, and 189-1171C-28X-4, 15 cm, and the stratigraphic distribution of nannofossils is given in Table **T4.** Key biohorizons are listed in Table **T6,** along with their sample interval and average depth. The Miocene sediments consist of nannofossil ooze, foraminifer-bearing nannofossil ooze, diatom-bearing nannofossil ooze, clay-bearing nannofossil ooze, nannofossil chalk, and foraminifer-bearing nannofossil chalk (Shipboard Scientific Party, 2001e). Calcareous nannofossils are abundant and moderately preserved in all samples.

The Miocene/Pliocene boundary (CN9/CN10) is placed between Samples 189-1171A-6H-7, 15 cm, and 7H-1, 15 cm (54.5 mbsf), based on the LO of *T. rugosus*. The base of the late Miocene *A. primus* CN9b Subzone was recognized based on the FO of *A. primus* at 65.57 mbsf. At the same depth, one sample contained rare *M. convallis*. Rare occurrences of *M. convallis* have been reported from Prydz Bay (Pospichal, 2002) and the South Atlantic at 42.5°S (Marino and Flores, 2002). The LO of *M. convallis* and the FO of *A. primus* indicate a brief hiatus across the CN9a/CN9b boundary. *Amaurolithus primus* was the only ceratolith recognized in Hole 1171A. The *A. primus* Subzone extends through Sample 189-1171A-8H-2, 15 cm, and is characterized by abundant *C. leptoporus, C. pelagicus, R. gelida, R. minuta, R. minutula, R. perplexa,* and *R. pseudoumbilicus*. The top of the *R. pseudoumbilicus* >7 µm paracme event occurs within this interval.

As at Sites 1168 and 1170, the *D. berggrenii* CN9a Subzone was combined with the *D. neorectus* CN8b Subzone. The base of this combined interval was approximated by the bottom of the *R. pseudoumbilicus* >7 µm paracme event, which occurs between Samples 189-1171A-9H-2, 15 cm, and 9H-3, 15 cm (76.0 mbsf). This interval contains abundant *C. leptoporus, C. pelagicus, R. gelida,* and *R. minutula*.

Late Miocene Zones CN8a, CN7, and CN6 were combined, as several marker species were absent from Site 1171 sediments. The base of the *C. coalitus* CN6 Zone is approximated by the LO of *C. miopelagicus* between Samples 189-1171C-16X-2, 15 m, and 16X-3, 15 cm (137.65 mbsf). The simultaneous LOs of *C. miopelagicus* and *C. floridanus* at 137.65 mbsf suggests that the CN5b *D. kugleri* Subzone is missing in Hole 1171C. Alternative explanations of the co-occurrence may be the spotty distribution of *C. miopelagicus* in Hole 1171C, the LOs at this site may be climatically rather than evolutionarily induced, or the LOs of these species are most likely diachronous (Wei and Wise, 1992; Raffi, et al, 1995; deKaenel and Villa, 1996; Backman and Raffi, 1997; Maiorano and Monechi, 1998). However unreliable these events may be, the interpretation of a hiatus at this depth is supported by diatom data (see **Stickley et al.,** this volume).

Sphenolithus heteromorphus was recorded in only one sample, and therefore the top of the *S. heteromorphus* Zone (CN4) is approximated by the LCO of *C. floridanus,* as in Hole 1170A. The CN4/CN5a boundary is placed between Samples 189-1171C-18X-5, 15 cm, and 18X-6, 15 cm (160.6 mbsf). Abundant *C. leptoporus, C. pelagicus, R. minuta, R. minutula,* and *R. pseudoumbilicus* were recorded in the CN5a *C. miopelagicus* Subzone. The LO of *C. premacintyrei* and the FOs of *R. gelida* and *R. perplexa* occurred within this interval.

As in Hole 1170A, the *S. heteromorphus* CN4 and the *H. ampliaperta* CN3 Zones are combined. The base of the combined CN3/CN4 Zone was roughly approximated by the FO of *C. premacintyrei,* as *S. heteromorphus* was rare and *S. belemnos* was not present in Hole 1171C. The base the combined zone is placed at 197.2 mbsf between Samples 189-1171C-22X-4, 15 cm, and 22X-5, 15 cm. *Calcidiscus leptoporus, C. pelagicus, C. floridanus, R. minuta,* and *R. minutula* are abundant throughout this interval. *Calcidiscus fuscus, C. premacintyrei, Discoaster* 6-rayed spp., *P. orangensis, R. haqii,* and *S. moriformis* were commonly recorded.

As at Site 1170, the base of the *S. belemnos* CN2 Zone could not be determined and CN2 was combined with the *D. druggii* CN1c Subzone. This combined zone contains abundant *C. pelagicus, C. floridanus, R. minuta,* and *R. minutula,* with commonly occurring *C. abisectus, Discoaster* 6-rayed spp., *P. orangensis, R. haqii,* and *S. moriformis*. A hiatus en-

compassing the early Miocene CN1a and CN1b Subzones is indicated by the FO of *C. tropicus* and the LO of *R. bisecta bisecta,* both at 253.47 mbsf (between Samples 189-1171C-28X-4, 15 cm, and 28X-CC). This interpretation of the O/M boundary is in agreement with other biostratigraphic data (**Stickley et al.,** this volume).

Hole 1172A

Hole 1172A (43°58′S, 149°70′E) was drilled in 2622 m water depth on the East Tasman Plateau (Fig. **F1**). Miocene sediments were recognized between Samples 189-1172A-8H-CC, and 37X-4, 15 cm, and the stratigraphic distribution of nannofossils is given in Table **T5.** Key biohorizons are listed in Table **T6,** along with their sample interval and average depth. The Miocene sediments consist of nannofossil ooze, nannofossil chalk, foraminifer-bearing nannofossil chalk, and nannofossil claystone (Shipboard Scientific Party, 2001f). Calcareous nannofossils were abundant and moderately preserved in all samples.

The Miocene/Pliocene boundary (CN9b/CN10) is tentatively placed between Samples 189-1172A-8H-CC, and 10H-3, 15 cm (79.34 mbsf), based on the combined LO of *D. quinqueramus* (5.53 Ma), used by Okada and Bukry (1980) to mark this boundary, and the LO of *T. rugosus* (5.23 Ma). This interval contained extremely disturbed cores, with large sections of flow-in (Scientific Shipboard Party, 2000f), making the exact placement of the Miocene/Pliocene boundary problematic (for further discussion see **Stickley et al.,** this volume). The interval from 189-1172A-10H-3, 15 cm, to 13H-7, 15 cm, represents the late Miocene *A. primus* CN9b Subzone, based on the FO of *A. primus*. Characteristic nannofossils of this zone are *A. primus, A. delicatus, C. leptoporus, R. minuta,* and *R. minutula*. The FO of *A. primus* and *A. delicatus* occur simultaneously with the top of the *R. pseudoumbilicus* >7 µm paracme and indicate a brief hiatus/condensed section at ~120 mbsf.

Several late and middle Miocene zones had to be combined in Hole 1172A, as key discoaster species were sporadically recorded or could not identified because of calcite overgrowth. Therefore, the *D. berggrenii* Subzone CN9a and the *D. neorectus* Subzone CN8b were combined and the base was approximated by the bottom of the *R. pseudoumbilicus* >7 µm paracme. This combined zone extends down to 163.7 mbsf (between Sample 189-1172A-18H-4, 15 cm, and 18H-5, 15 cm) and is characterized by the low abundance of *R. pseudoumbilicus* >7 µm and the presence of *C. leptoporus, C. pelagicus, R. minuta, R. minutula,* and *R. perplexa*. Low numbers of *C. macintyrei, Discoaster* spp. 6-rayed, *S. moriformis* <6 µm, and *T. rugosus* are present in this interval.

Discoaster hamatus, C. calyculus, C. coalitus, and *M. convallis* were not recorded in Hole 1172A sediments, causing the combination of the late Miocene *D. bellus* CN8a, the middle Miocene *D. hamatus* CN7, and the *C. coalitus* CN6 Zones. The base of Zone CN6 is estimated by the LO of *C. miopelagicus* between Sample 189-1172A-26X-3, 15 cm, and 26X-4, 15 cm (234.0 mbsf). This interval is characterized by common to abundant *C. leptoporus, C. pelagicus, R. gelida, R. minutula,* and *R. perplexa*.

The base the *D. kugleri* CN5b Subzone is marked by the LO of *C. floridanus* between Samples 189-1172A-27X-3, 15 cm, and 27X-4, 15 cm (243.6 mbsf). This short interval contains common *C. leptoporus, C. pelagicus, R. minutula, R. pseudoumbilicus,* and abundant *R. gelida*.

The LO of *S. heteromorphus* is placed in Sample 189-1172A-31X-3, 15 cm (281.5 mbsf), marking the base of the *C. miopelagicus* CN5a Subzone. This subzone is dominated by *C. leptoporus, C. pelagicus, R.*

pseudoumbilicus, R. gelida, R. minuta, and *R. minutula*. Scarce to rare nannofossils are represented by *C. macintyrei, C. miopelagicus, Discoaster* spp. 6-rayed, *G. rotula, P. hermosus, R. haqii,* and *S. compactus*. The LO of *C. premacintyrei* (12.7 Ma) and the LCO of *C. floridanus* (13.2 Ma) occur within this interval.

The *S. heteromorphus* CN4 and the *H. ampliaperta* CN3 Zones were combined, as *H. ampliaperta* was not recorded in Hole 1172A. The base of this combined zone is marked by the FO of *S. heteromorphus* between Samples 189-1172A-34X-4, 15 cm, and 34X-5, 15 cm (311.9 mbsf). *Cyclicargolithus floridanus, Discoaster* spp. 6 rayed, *R. haqii,* and *R. minutula* are common to abundant throughout this interval.

Sphenolithus belemnos, which marks the base of the *S. belemnos* CN2 Zone was not recorded in Hole 1172A. This suggests that the CN2 Zone is not present in Hole 1172A and that a hiatus encompassing the *S. belemnos* CN2 Zone exists. It is possible that *S. belemnos* was ecologically excluded from Site 1172 as at Sites 1170 and 1171. In the absence of corroborating data from other microfossil groups or magnetostratigraphy for a hiatus and as the ecological requirements of this extinct species are not well known, the author assumes that no hiatus exists.

The early Miocene *T. carinatus* Zone is subdivided based on the FO of *C. tropicus*. This occurs between Samples 189-1172A-36X-4, 15 cm, and 36X-5, 15 cm, and is used to approximate the CN1b/CN1c boundary. A hiatus is suggested at this depth by the co-occurrence of *C. tropicus* and two early Miocene planktonic foraminifers (for details see **Stickley et al.,** this volume). The early Miocene sediments are characterized by abundant to common *C. pelagicus, C. floridanus, Discoaster* 6-rayed, *R. haqii, R. minuta, R. minutula,* and *S. compactus*. The Oligocene/Miocene boundary (CP19/CN1) is placed at 340.46 mbsf between Samples 189-1172A-37X-4, 15 cm, and 37X-4, 117 cm, based on the LO of *R. bisecta bisecta*.

SUMMARY

Distribution of calcareous nannofossils at Sites 1168, 1170, 1171, and 1172 was obtained by semiquantitative analyses. Diversity of nannofossils at Site 1168 was sufficient to allow the recognition of most Okada and Bukry (1980) Miocene zones. In comparison, at the other three sites, diversity was lower and resulted in less biostratigraphic resolution. Despite the low abundance of some marker species within the triquetrorhabdulids, ceratoliths, and sphenoliths, a reliable biostratigraphy could be generated from their abundance patterns when compared with stratigraphic data available from foraminiferal, diatom, radiolarian, and magnetostratigraphies.

Several alternative markers were used to help refine the stratigraphy of Leg 189 sites. The top and bottom of the *R. pseudoumbilicus* >7 µm paracme, the FO of *C. premacintyrei,* and the FO of *C. tropicus* appear to be useful events in the Tasman Seaway. Additional quantitative work would provide a detailed view of the distribution of these species.

Core disturbance and extreme bioturbation in the upper Miocene and across the Miocene/Pliocene boundary at Sites 1170, 1171, and 1172 complicated the interpretation of the sedimentary history of these regions. Overgrowth of delicate features on sphenoliths in the lower Miocene and on discoasters in the upper Miocene sections prevented the identification of the complete range of *Sphenolithus disbelemnos, Sphenolithus dissimilis, D. loeblichii,* and *D. surculus*.

ACKNOWLEGMENTS

We thank the Ocean Drilling Program and the crew of the *JOIDES Resolution* for a marvelous cruise. We thank Isabella Raffi for a thoughtful review, which helped to improve the manuscript. Katie Lott deserves a thank you for preparation of the slides used in this study. This research used samples and data provided by the Ocean Drilling Program (ODP). ODP is sponsored by the U.S. National Science Foundation (NSF) and participating countries under management of Joint Oceanographic Institutions (JOI), Inc. Funding for this research was provided by USSAC funds to Kristeen L. McGonigal. Laboratory facilities were provided by NSF grant DPP 94-22893.

REFERENCES

Backman, J., and Raffi, I., 1997. Calibration of Miocene nannofossil events to orbitally tuned cyclostratigraphies from Ceara Rise. *In* Shackleton, N.J., Curry, W.B., Richter, C., and Bralower, T.J. (Eds.), *Proc. ODP, Sci. Results,* 154: College Station, TX (Ocean Drilling Program), 83–99.

Berggren, W.A., Kent, D.V., Swisher, C.C., III, and Aubry, M.-P., 1995. A revised Cenozoic geochronology and chronostratigraphy. *In* Berggren, W.A., Kent, D.V., Aubry, M.-P., and Hardenbol, J. (Eds.), *Geochronology, Time Scales and Global Stratigraphic Correlation*. Spec. Publ.—SEPM, 54:129–212.

Bown, P.R. (Ed.), 1998. *Calcareous Nannofossil Biostratigraphy:* London (Chapman-Hall).

de Kaenel, E., and Villa, G., 1996. Oligocene–Miocene calcareous nannofossils biostratigraphy and paleoecology from the Iberia Abyssal Plain. *In* Whitmarsh, R.B., Sawyer, D.S., Klaus, A., and Masson, D.G. (Eds.), *Proc. ODP, Sci. Results,* 149: College Station, TX (Ocean Drilling Program), 79–145.

Gartner, S., 1992. Miocene nannofossil chronology in the North Atlantic, DSDP Site 608. *Mar. Micropaleontol.,* 18:307–331.

Maiorano, P., and Monechi, S., 1998. Revised correlation of early and middle Miocene calcareous nannofossil events and magnetostratigraphy from DSDP Site 563 (North Atlantic Ocean). *Mar. Micropaleontol.,* 35:235–255.

Marino, M., and Flores, J.A., 2002. Data report: Calcareous nannofossil stratigraphy at Sites 1088 and 1090 (ODP Leg 177, Southern Ocean). *In* Gersonde, R., Hodell, D.A., and Blum, P. (Eds.), *Proc. ODP, Sci. Results,* 177, 1–14 [CD-ROM]. Available from: Ocean Drilling Program, Texas A&M University, College Station TX 78745-9547, USA.

Martini, E., 1971. Standard Tertiary and Quaternary calcareous nannoplankton zonation. *In* Farinacci, A. (Ed.), *Proc. 2nd Int. Conf. Planktonic Microfossils Roma:* Rome (Ed. Tecnosci.), 2:739–785.

Okada, H., and Bukry, D., 1980. Supplementary modification and introduction of code numbers to the low-latitude coccolith biostratigraphic zonation (Bukry, 1973; 1975). *Mar. Micropaleontol.,* 5:321–325.

Olafsson, G., 1989. Quantitative calcareous nannofossil biostratigraphy of upper Oligocene to middle Miocene sediment from ODP Hole 667A and middle Miocene sediment from DSDP Site 574. *In* Ruddiman, W., Sarnthein, M., et al., *Proc. ODP, Sci. Results,* 108: College Station, TX (Ocean Drilling Program), 9–22.

Perch-Nielsen, K., 1985. Cenozoic calcareous nannofossils. *In* Bolli, H.M., Saunders, J.B., and Perch-Nielsen, K. (Eds.), *Plankton Stratigraphy:* Cambridge (Cambridge Univ. Press), 427–554.

Pospichal, J.J., 2002. Speculations on the occurrence of the late Miocene species, *Minylitha convallis*, in Antarctic margin sediments. *J. Nannoplankton Res.,* 24:195–197.

Raffi, I., Backman, J., and Rio, D., 1998. Evolutionary trends of calcareous nannofossils in the Late Neogene. *Mar. Micropaleontol.,* 35:17–41.

Raffi, I., and Flores, J.-A., 1995. Pleistocene through Miocene calcareous nannofossils from eastern equatorial Pacific Ocean. *In* Pisias, N.G., Mayer, L.A., Janecek, T.R., Palmer-Julson, A., and van Andel, T.H. (Eds.), *Proc. ODP, Sci. Results,* 138: College Station, TX (Ocean Drilling Program), 233–286.

Raffi, I., Rio, D., d'Atri, A., Fornaciari, E., and Rocchetti, S., 1995. Quantitative distribution patterns and biomagnetostratigraphy of middle and late Miocene calcareous nannofossils from equatorial Indian and Pacific oceans (Leg 115, 130, and 138). *In* Pisias, N.G., Mayer, L.A., Janecek, T.R., Palmer-Julson, A., and van Andel, T.H. (Eds.), *Proc. ODP, Sci. Results,* 138: College Station, TX (Ocean Drilling Program), 479–502.

Shackleton, N.J., Hall, M.A., Raffi, I., Tauxe, L., and Zachos, J., 2000. Astronomical calibration age for the Oligocene/Miocene boundary. *Geology,* 28:447–450.

Shipboard Scientific Party, 2001a. Leg 189 summary. *In* Exon, N.F., Kennett, J.P., Malone, M.J., et al., *Proc. ODP, Init. Repts.,* 189, 1–98 [CD-ROM]. Available from: Ocean Drilling Program, Texas A&M University, College Station TX 77845-9547, USA.

————, 2001b. Site 1168. *In* Exon, N.F., Kennett, J.P., Malone, M.J., et al., *Proc. ODP, Init. Repts.,* 189, 1–170 [CD-ROM]. Available from: Ocean Drilling Program, Texas A&M University, College Station TX 77845-9547, USA.

————, 2001c. Site 1169. *In* Exon, N.F., Kennett, J.P., Malone, M.J., et al., *Proc. ODP, Init. Repts.,* 189, 1–64 [CD-ROM]. Available from: Ocean Drilling Program, Texas A&M University, College Station TX 77845-9547, USA.

————, 2001d. Site 1170. *In* Exon, N.F., Kennett, J.P., Malone, M.J., et al., *Proc. ODP, Init. Repts.,* 189, 1–167 [CD-ROM]. Available from: Ocean Drilling Program, Texas A&M University, College Station TX 77845-9547, USA.

————, 2001e. Site 1171. *In* Exon, N.F., Kennett, J.P., Malone, M.J., et al., *Proc. ODP, Init. Repts.,* 189, 1–176 [CD-ROM]. Available from: Ocean Drilling Program, Texas A&M University, College Station TX 77845-9547, USA.

————, 2001f. Site 1172. *In* Exon, N.F., Kennett, J.P., Malone, M.J., et al., *Proc. ODP, Init. Repts.,* 189, 1–149 [CD-ROM]. Available from: Ocean Drilling Program, Texas A&M University, College Station TX 77845-9547, USA.

Wei, W., and Wise, S.W., Jr., 1992. Selected Neogene calcareous nannofossil index taxa of the Southern Ocean: biochronology, biometrics, and paleoceanography. *In* Wise, S.W., Jr., Schlich, R., et al., *Proc. ODP, Sci. Results,* 120: College Station, TX (Ocean Drilling Program), 523–537.

Young, J.R., 1998. Neogene. *In* Bown, P.R. (Ed.), *Calcareous Nannofossil Biostratigraphy* (Vol. 8): Dordrecht (Kluwer Academic), 225–265.

APPENDIX

Calcareous nannofossils considered in this report are listed in Table AT1 and are illustrated in Plates P1, P2, P3, P4, P5, P6, P7, P8, P9, P10, P11, P12, and P13.

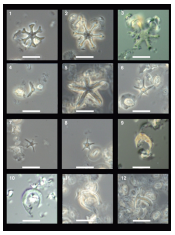

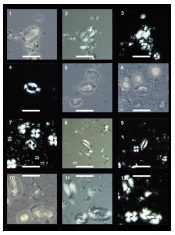

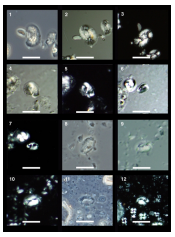

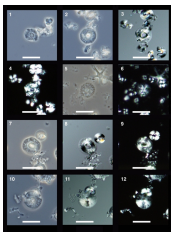

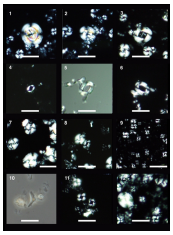

Figure F1. Location map of Leg 189 Sites 1168, 1169, 1170, 1171, and 1172 in the offshore Tasmanian region. The contours of the regional bathymetric chart are 500-m intervals.

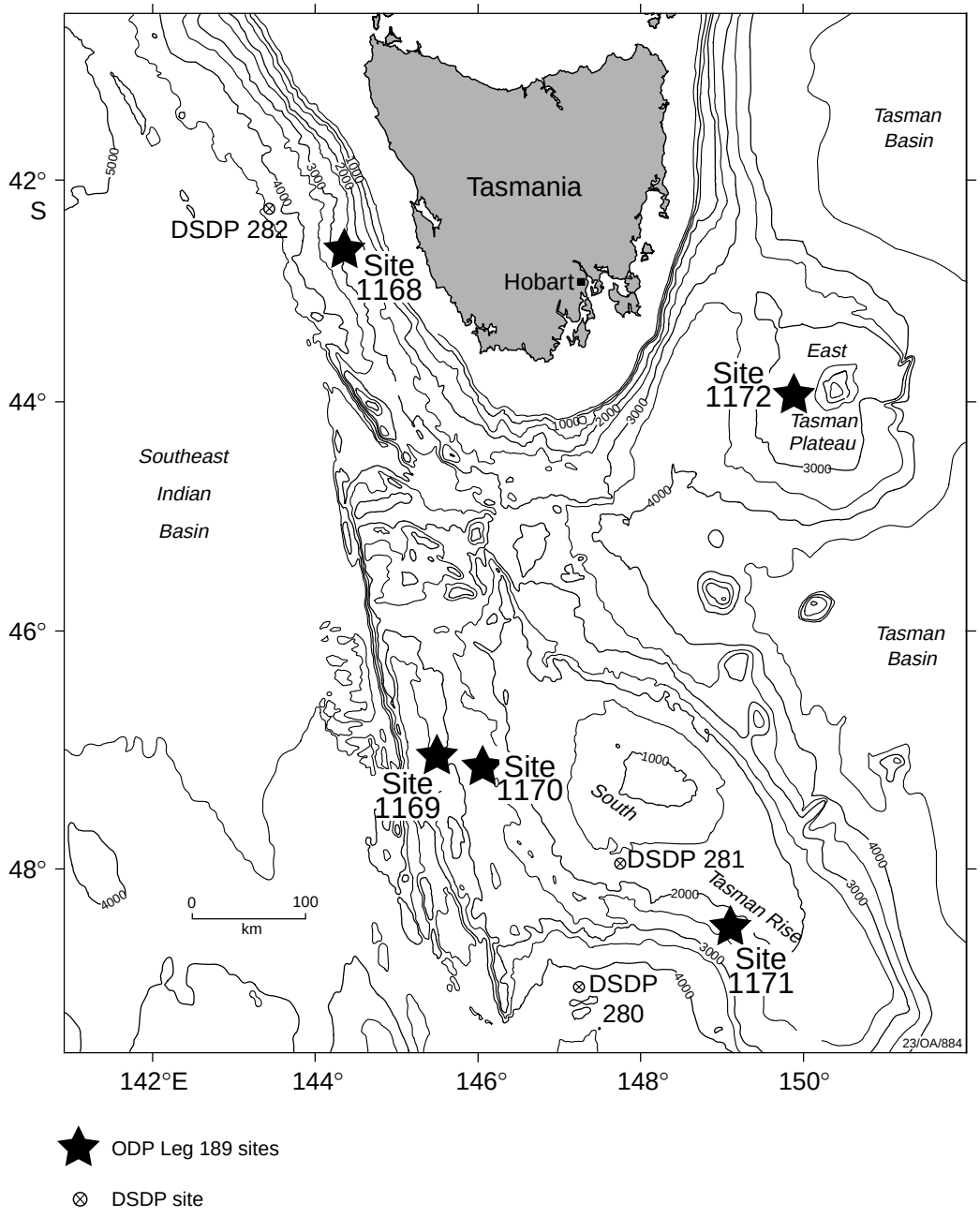

Figure F2. Summary of nannofossil zones and datums used in this study with the geomagnetic scale of Berggren, et al. (1995). See Table T6, p. 22, for biochronology sources (FO = first occurrence, LO = last occurrence, LCO = last common occurrence, B = bottom of paracme event, T = top of paracme event).

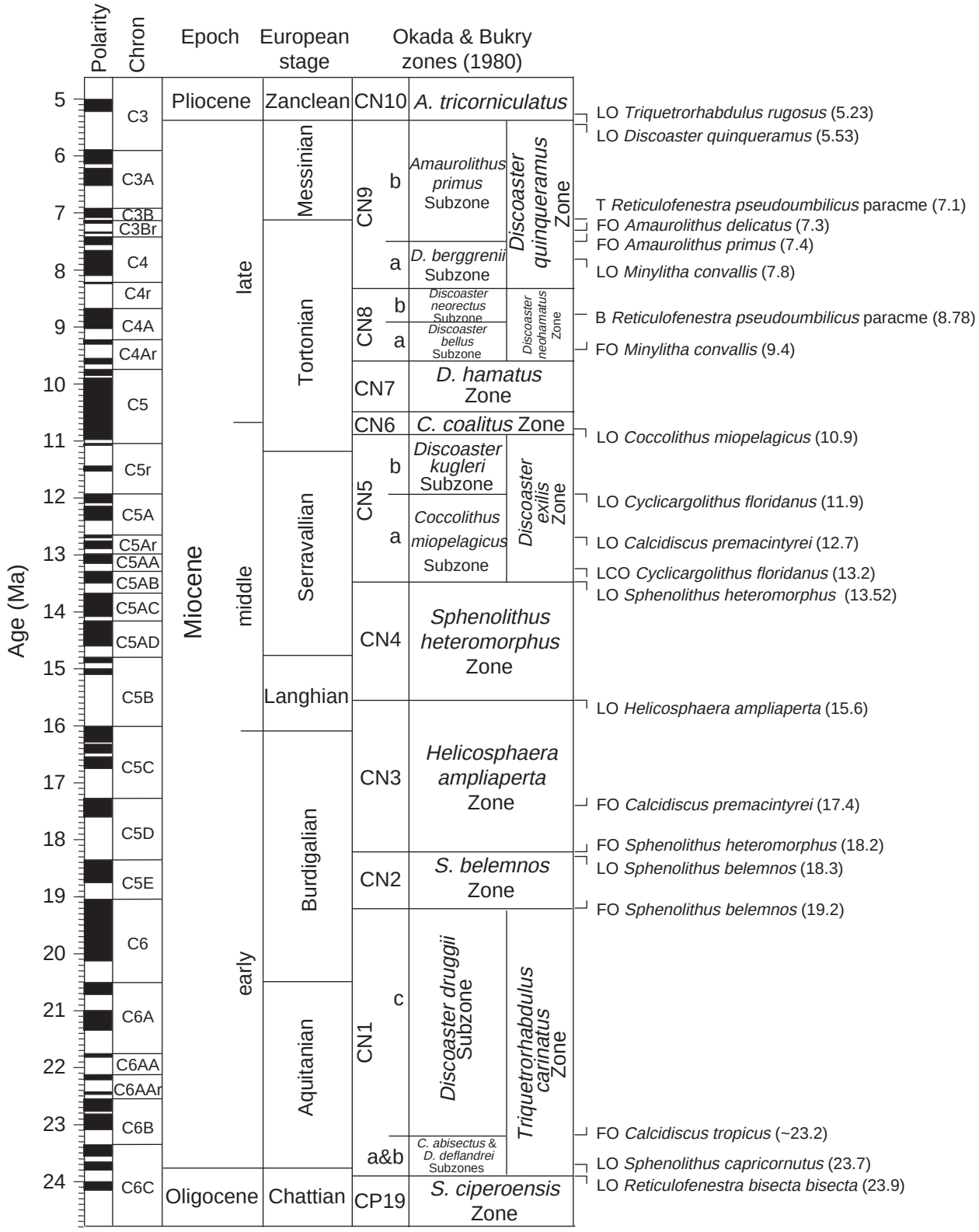

Table T1. Semiquantitative stratigraphic distribution of calcareous nannofossils, Hole 1168A. (This table is available in an **oversized format** and in **ASCII.**)

Table T2. Quantitative stratigraphic distribution of calcareous nannofossils across the Oligocene/Miocene boundary, Hole 1168A. (This table is available in an **oversized format** and in **ASCII.**)

Table T3. Semiquantitative stratigraphic distribution of Miocene calcareous nannofossils, Hole 1170A. (This table is available in an **oversized format** and in **ASCII.**)

Table T4. Semiquantitative stratigraphic distribution of Miocene calcareous nannofossils, Holes 1171A and 1171C. (This table is available in an **oversized format** and in **ASCII.**)

Table T5. Semiquantitative stratigraphic distribution of Miocene calcareous nannofossils, Hole 1172A. (This table is available in an **oversized format** and **ASCII.**)

Table T6. Miocene calcareous nannofossil events. (**See table notes.** Continued on next page.)

Age (Ma)	Event	Top		Bottom		Mean depth (mbsf)	Error (± m)	Reference
		Core, section, interval (cm)	Depth (mbsf)	Core, section, interval (cm)	Depth (mbsf)			
		189-1168A-		189-1168A-				
5.23	LO *Triquetrorhabdulus rugosus*	10H-1, 15	83.45	10H-2, 16	84.95	84.20	0.75	1
7.1	T *Reticulofenestra pseudoumbilicus* paracme	12H-1, 15	102.45	12H-2, 15	103.95	103.20	0.75	1
7.3	FO *Amaurolithus delicatus*	12H-3, 15	105.45	12H-4, 15	106.95	106.20	0.75	2
7.4	FO *Amaurolithus primus*	12H-6, 15	109.95	12H-7, 15	111.45	110.70	0.75	2
7.8	LO *Minylitha convallis*	15X-1, 15	128.25	15X-2, 15	129.75	129.00	0.75	3
8.78	B *Reticulofenestra pseudoumbilicus* paracme	15X-2, 15	129.75	15X-3, 15	131.25	130.50	0.75	1
9.4	FO *Minylitha convallis*	17X-4, 15	151.95	17X-5, 15	153.45	152.70	0.75	3
10.94	LO *Calcidiscus miopelagicus*	20X-5, 15	182.25	20X-6, 15	183.75	183.00	0.75	1
11.9	LO *Cyclicargolithus floridanus*	22X-2, 15	197.05	22X-3, 15	198.55	197.80	0.75	4
12.7	LO *Calcidiscus premacintyrei*	24X-5, 15	220.75	24X-6, 15	222.25	221.50	0.75	5
13.2	LCO *Cyclicargolithus floridanus*	26X-2, 15	235.45	26X-3, 15	236.95	236.20	0.75	6
13.52	LO *Sphenolithus heteromorphus*	26X-6, 15	241.45	26X-7, 15	242.95	242.20	0.75	1
17.4	FO *Calcidiscus premacintyrei*	30X-6, 15	279.85	30X-7, 15	280.85	280.35	0.50	4
18.2	FO *Sphenolithus heteromorphus*	32X-2, 15	293.05	32X-3, 15	294.55	293.80	0.75	3
18.3	LO *Sphenolithus belemnos*	32X-6, 15	299.05	32X-7, 15	300.05	299.55	0.50	3
19.2	FO *Sphenolithus belemnos*	34X-3, 15	313.15	34X-4, 15	314.65	313.90	0.75	3
22.3	LO *Ilselithina fusa*	41X-3, 2	380.32	41X-3, 40	380.70	380.51	0.19	4
~23.2	FO *Calcidiscus tropicus*	43X-5, 2	402.52	43X-5, 40	402.90	402.71	0.19	7
23.7	LO *Sphenolithus capricornutus*	47X-2, 78	437.18	47X-2, 120	437.60	437.39	0.21	3
23.8	LO *Sphenolithus delphix*	47X-3, 59	438.49	47X-3, 78	438.68	438.59	0.09	8
23.9	LO *Reticulofenestra bisecta bisecta*	47X-4, 40	439.80	47X-4, 68	440.08	439.94	0.14	3
24.3	FO *Sphenolithus delphix*	48X-3, 138	448.88	48X-4, 2	449.02	448.95	0.07	8
		189-1170A-		189-1170A-				
5.23	LO *Triquetrorhabdulus rugosus*	15H-3, 60	128.32	15H-4, 60	130.32	129.32	1.00	1
7.1	T *Reticulofenestra pseudoumbilicus* paracme	17H-6, 60	152.11	19X-1, 60	163.80	157.96	5.85	1
7.3	FO *Amaurolithus delicatus*	17H-CC	153.57	19X-1, 60	163.80	158.69	5.12	2
7.4	FO *Amaurolithus primus*	17H-CC	153.57	19X-1, 60	163.80	158.69	5.12	2
8.78	B *Reticulofenestra pseudoumbilicus* paracme	21X-2, 60	178.40	21X-3, 60	179.90	179.15	0.75	1
10.94	LO *Coccolithus miopelagicus*	25X-2, 60	216.80	25X-3, 60	218.30	217.55	0.75	1
11.9	LO *Cyclicargolithus floridanus*	28X-4, 60	248.60	28X-5, 60	250.10	249.35	0.75	4
12.7	LO *Calcidiscus premacintyrei*	30X-5, 60	269.30	31X-1, 60	272.90	271.10	1.80	5
13.2	LCO *Cyclicargolithus floridanus*	31X-4, 60	277.40	31X-5, 60	278.90	278.15	0.75	6
17.4	FO *Calcidiscus premacintyrei*	35X-2, 60	312.20	35X-3, 60	313.70	312.95	0.75	4
~23.2	FO *Calcidiscus tropicus*	42X-3, 110	381.50	42X-4, 60	383.00	382.25	0.75	7
23.9	LO *Reticulofenestra bisecta bisecta*	42X-3, 110	381.50	42X-4, 60	383.00	382.25	0.75	3
		189-1171A-		189-1171A-				
5.23	LO *Triquetrorhabdulus rugosus*	6H-7, 15	54.25	7H-1, 15	54.75	54.50	0.25	1
7.1	T *Reticulofenestra pseudoumbilicus* paracme	7H-7, 15	63.75	8H-1, 15	64.25	64.00	0.25	1
7.4	FO *Amaurolithus primus*	8H-2, 15	65.25	8H-3, 15	65.89	65.57	0.32	2
7.8	LO *Minylithus convallis*	8H-2, 15	65.25	8H-3, 15	65.89	65.57	0.32	3
8.78	B *Reticulofenestra pseudoumbilicus* paracme	9H-2, 15	75.25	9H-3, 15	76.75	76.00	0.75	1
		189-1171C-		189-1171C-				
10.94	LO *Coccolithus miopelagicus*	16X-2, 15	136.15	16X-3, 15	137.65	136.90	0.75	1
11.9	LO *Cyclicargolithus floridanus*	16X-2, 15	136.15	16X-3, 15	137.65	136.90	0.75	4
12.7	LO *Calcidiscus premacintyrei*	17X-1, 15	144.25	17X-2, 15	145.75	145.00	0.75	5
13.2	LCO *Cyclicargolithus floridanus*	18X-5, 15	159.85	18X-6, 15	161.35	160.60	0.75	6

Table T6 (continued).

Age (Ma)	Event	Top		Bottom		Mean depth (mbsf)	Error (± m)	Reference
		Core, section, interval (cm)	Depth (mbsf)	Core, section, interval (cm)	Depth (mbsf)			
17.4	FO *Calcidiscus premacintyrei*	22X-4, 15	196.45	22X-5, 15	197.95	197.20	0.75	4
~23.2	FO *Calcidiscus tropicus*	28X-4, 15	252.15	28X-CC	252.79	252.47	0.32	7
23.9	LO *Reticulofenestra bisecta bisecta*	28X-4, 15	252.15	28X-CC	252.79	252.47	0.32	3
		189-1172A-		189-1172A-				
5.23	LO *Triquetrorhabdulus rugosus*	8H-CC	73.22	10H-3, 15	85.45	79.34	6.12	1
5.53	LO *Discoaster quinqueramus*	8H-CC	73.22	10H-3, 15	85.45	79.34	6.12	1
7.1	T *Reticulofenestra pseudoumbilicus* paracme	13H-7, 15	119.95	14H-1, 15	121.47	120.71	0.76	1
7.3	FO *Amaurolithus delicatus*	13H-7, 15	119.95	14H-1, 15	121.47	120.71	0.76	2
7.4	FO *Amaurolithus primus*	13H-7, 15	119.95	14H-1, 15	121.47	120.71	0.76	2
8.78	B *Reticulofenestra pseudoumbilicus* paracme	18H-4, 15	162.95	18H-5, 15	164.45	163.70	0.75	1
10.94	LO *Coccolithus miopelagicus*	26X-3, 15	233.25	26X-4, 15	234.75	234.00	0.75	1
11.9	LO *Cyclicargolithus floridanus*	27X-3, 15	242.85	27X-4, 15	244.35	243.60	0.75	4
12.7	LO *Calcidiscus premacintyrei*	30X-4, 15	272.17	30X-5, 15	274.15	273.16	0.99	5
13.2	LCO *Cyclicargolithus floridanus*	30X-5, 15	274.15	30X-6, 15	275.65	274.90	0.75	6
13.52	LO *Sphenolithus heteromorphus*	31X-3, 15	280.75	31X-4, 15	282.25	281.50	0.75	1
17.4	FO *Calcidiscus premacintyrei*	34X-2, 15	308.15	34X-3, 15	309.85	309.00	0.85	4
18.2	FO *Sphenolithus heteromorphus*	34X-4, 15	311.15	34X-5, 15	312.65	311.90	0.75	3
~23.2	FO *Calcidiscus tropicus*	36X-4, 15	330.35	36X-5, 15	331.85	331.10	0.75	7
23.9	LO *Reticulofenestra bisecta bisecta*	37X-4, 15	339.95	37X-4, 117	340.97	340.46	0.51	3

Notes: LO = last occurrence, FO = first occurrence, LCO = last common occurrence. T = top of event, B = bottom of event. References: 1 = Backman and Raffi, 1997; 2 = Raffi et al., 1998; 3 = Berggren et al., 1995; 4 = Gartner, 1992; 5 = Maiorano and Monechi, 1998; 6 = Raffi et al., 1995; 7 = de Kaenel and Villa, 1996; 8 = Shackleton et al., 2000. This table is also available in **ASCII.**

Plate P1. Scale bar = 10 µm. **1.** *Discoaster bellus* (Sample 189-1172A-18H-7, 15 cm) (phase-contrast light [Ph]). **2, 3.** *Discoaster* sp. 5-ray (Sample 189-1172A-13H-6, 15 cm); (2) Ph; (3) differential-interference contrast light (DIC). **4.** *Discoaster challengeri* (Sample 189-1172A-18H-7, 15 cm) (Ph). **5.** *Discoaster exilis* (Sample 189-1172A-12H-6, 15 cm) (Ph). **6.** *Discoaster extensus* (Sample 189-1168A-11H-3, 15 cm) (Ph). **7.** *Discoaster braarudii* (Sample 189-1172A-10H-3, 117 cm) (Ph). **8.** *Discoaster deflandrei* (Sample 189-1170A-38X-2, 60 cm) (DIC). **9.** *Discoaster* spp. (Sample 189-1170A-40X-1, 60 cm) (DIC). **10–12.** *Catinaster coalitus* (Sample 189-1168A-19X-1, 15 cm); (10) Ph; (11) DIC; (12) polarized light.

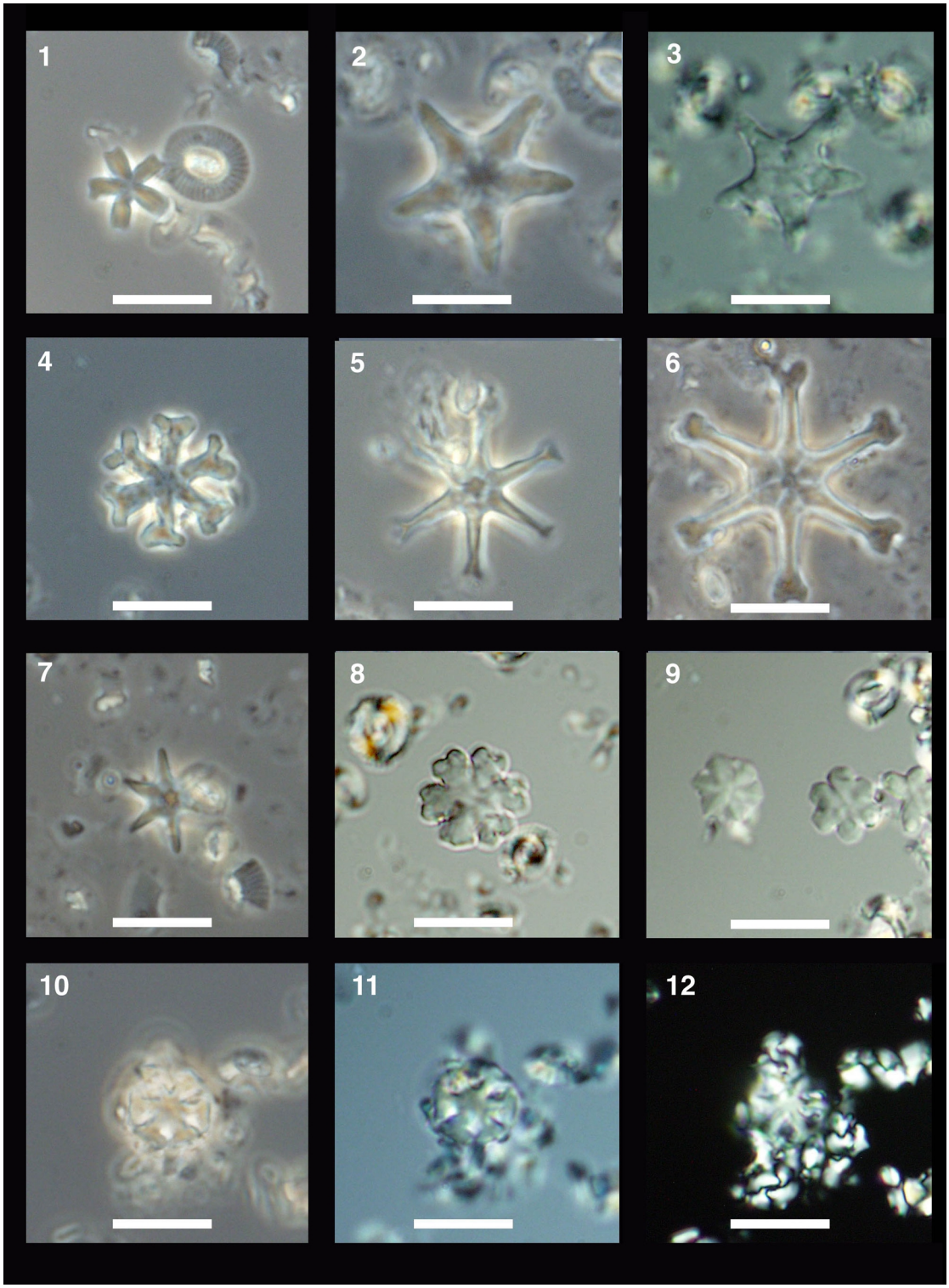

Plate P2. Scale bar = 10 µm. **1.** *Discoaster loeblichii* (Sample 189-1172A-10H-3, 15 cm) (phase-contrast light [Ph]). **2, 3.** *Discoaster surculus* (Sample 189-1172A-10H-3, 15 cm); (2) Ph; (3) differential-interference contrast light (DIC). **4.** *Discoaster triradiatus* (Sample 189-1172A-10H-3, 117 cm) (Ph). **5.** *Discoaster hamatus* (Sample 189-1172A-20H-7, 15 cm) (Ph). **6, 7.** *Discoaster quinqueramus* (6) Sample 1172A-12H-6, 15 cm (Ph); (7) Sample 189-1172A-10H-3, 15 cm (Ph). **8.** *Discoaster berggrenii*? (Sample 189-1172A-10H-3, 15 cm) (Ph). **9.** *Amaurolithus primus* (Sample 189-1172A-12H-5, 15 cm) (Ph). **10.** *Amaurolithus delicatus* (Sample 189-1170A-15H-3, 60 cm) (DIC). **11.** *Amaurolithus ninae* (Sample 189-1172A-11H-7, 15 cm) (Ph). **12.** *Amaurolithus triconiculatus* (Sample 189-1172A-11H-7, 15 cm) (Ph).

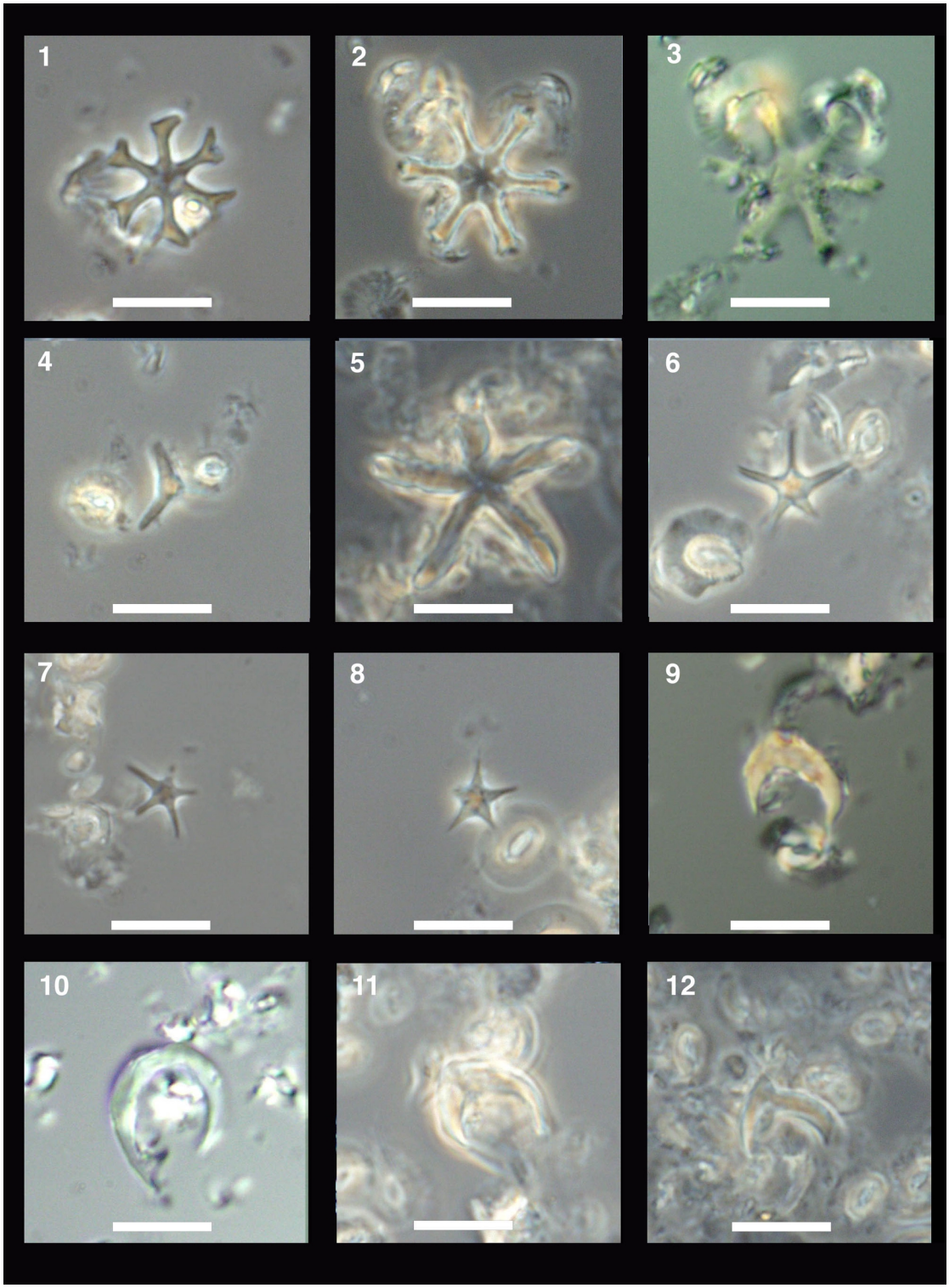

Plate P3. Scale bar = 10 µm. **1–4.** *Helicosphaera ampliaperta* (Sample 189-1170A-31X-5, 60 cm); (1) phase-contrast light (Ph); (2) differential-interference contrast light (DIC); (3, 4) polarized light (XP). **5–7.** *Helicosphaera recta* (Sample 189-1168A-47X-3, 40 cm); (5, 6) Ph; (7) XP. **8, 9.** *Helicosphaera elongata* (Sample 189-1168A-38X-1, 15 cm); (8) Ph; (9) XP. **10–12.** *Helicosphaera paleocarteri, Cyclicargolithus floridanus,* and *Helicosphaera euphratis* (Sample 1168A-38X-4, 15 cm); (10) Ph; (11) DIC; (12) XP.

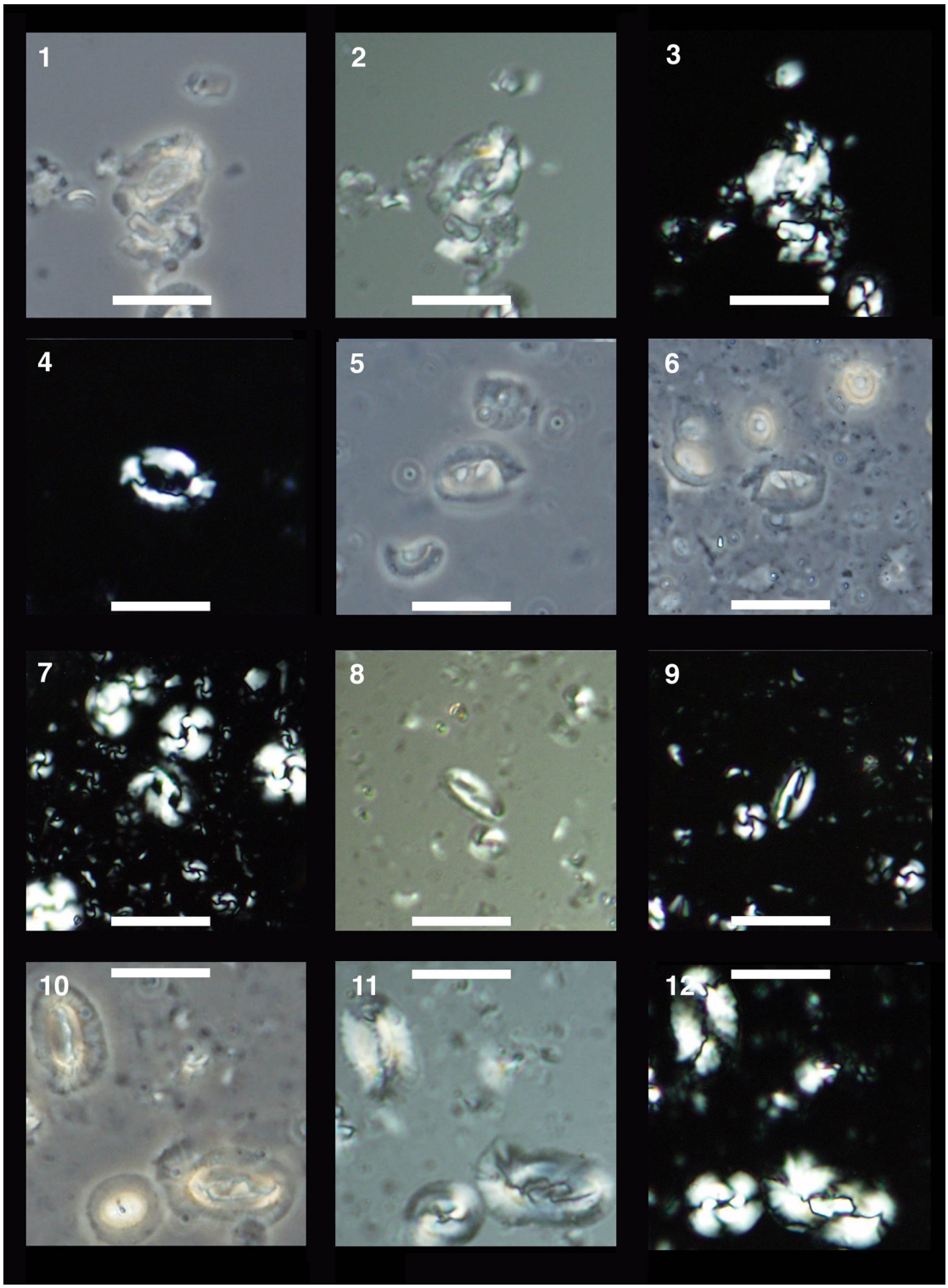

Plate P4. Scale bar = 10 µm. **1–3.** *Helicosphaera paleocarteri* (Sample 189-1171C-20X-6, 15 cm); (1) phase-contrast light (Ph); (2) differential-interference contrast light (DIC); (3) polarized light (XP). **4–7.** *Helicosphaera compacta;* (4, 5) Sample 189-1168A-41X-5, 2 cm; (4) Ph; (5) XP; (6, 7) Sample 189-1168A-44X-2, 80 cm; (6) DIC; (7) XP. **8–10.** *Helicosphaera obliqua* (Sample 189-1168A-28X-5, 15 cm); (8) Ph; (9) DIC; (10) XP. **11, 12.** *Helicosphaera perch-nielsenae* (Sample 189-1168A-46X-7, 15 cm); (11) Ph; (12) XP.

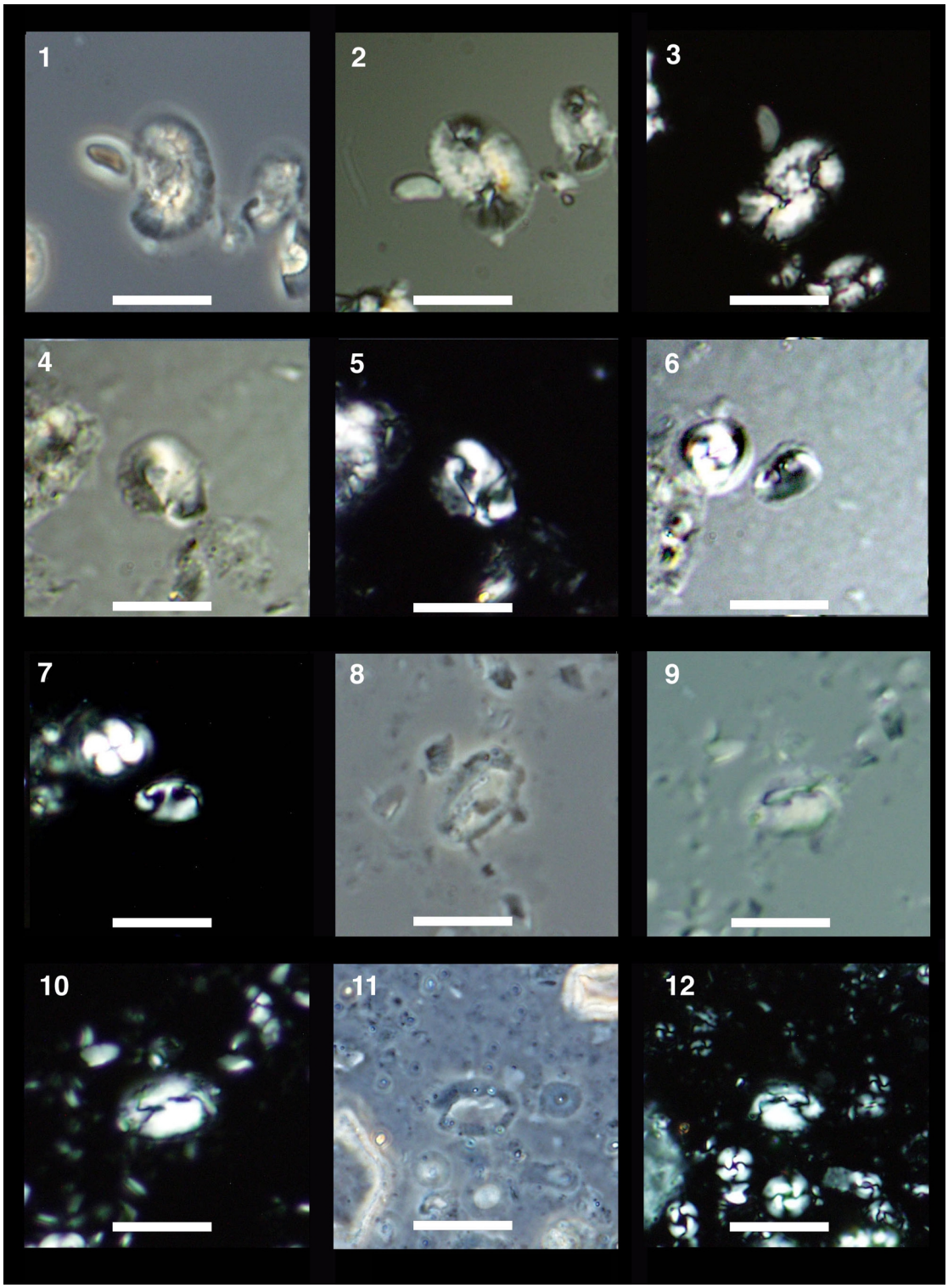

Plate P5. Scale bar = 10 µm. **1.** *Calcidiscus radiatus* (Sample 189-1171C-22X-3, 15 cm) (phase-contrast light [Ph]). **2–4.** *Calcidiscus tropicus* (Sample 189-1171C-17X-3,15 cm); (2) Ph; (3) differential-interference contrast light (DIC); (4) polarized light (XP). **5, 6.** *Calcidiscus leptoporus* (Sample 189-1172A-10H-3, 15 cm); (5) Ph; (6) XP. **7–9.** *Calcidiscus premacintyrei* (Sample 189-1171C-22X-4, 15 cm); (7) Ph; (8) DIC; (9) XP. **10–12.** *Calcidiscus macintyrei* (Sample 189-1171C-16X-3, 15 cm); (10) Ph; (11) DIC; (12) XP.

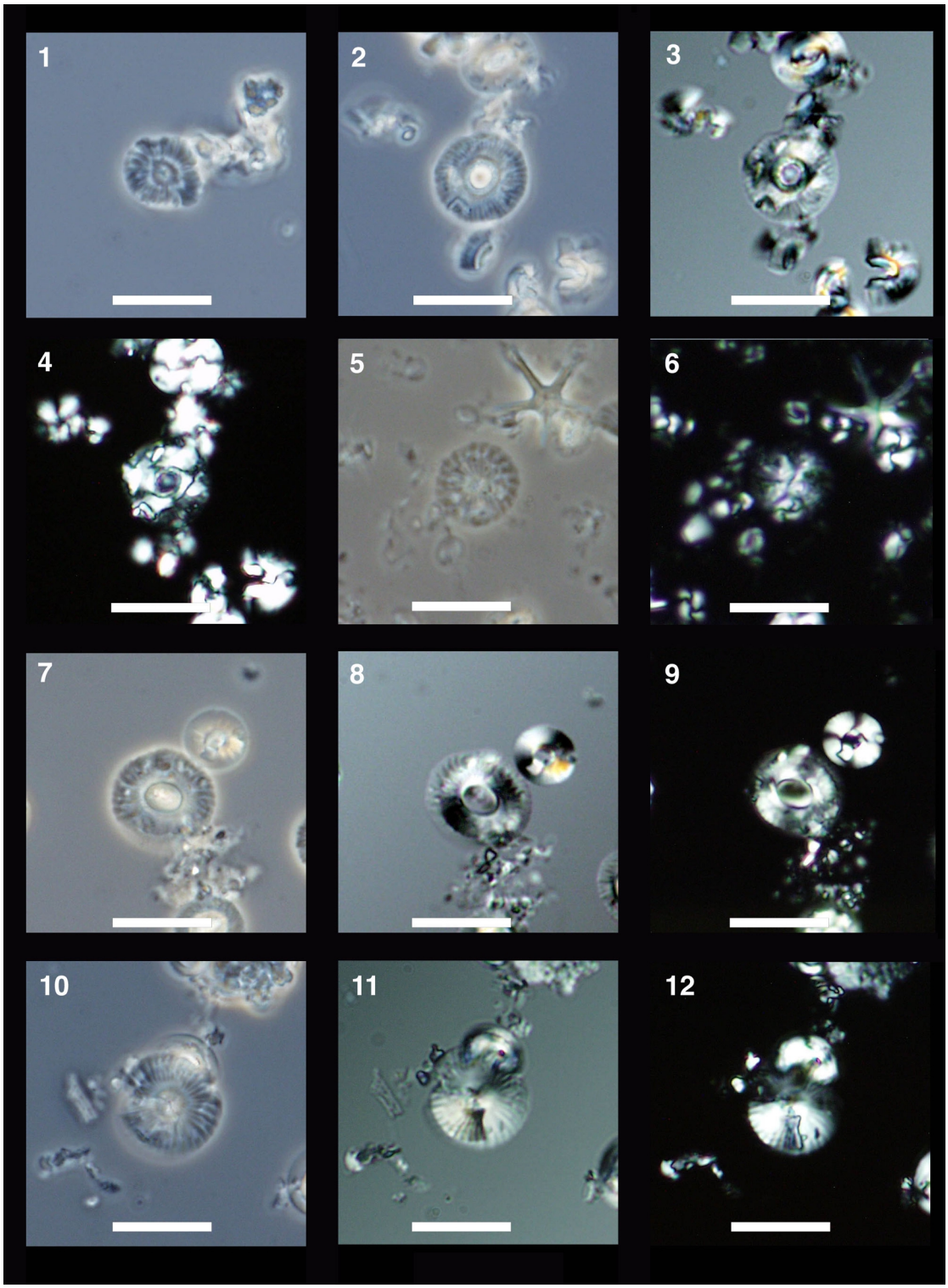

Plate P6. Scale bar = 10 µm. **1.** *Reticulofenestra stavensis* (Sample 189-1171C-29X-1, 117 cm) (polarized light [XP]). **2.** *Reticulofenestra bisecta bisecta* (Sample 189-1171C-29X-1, 117 cm) (XP). **3.** *Reticulofenestra lockerii* (Sample 189-1168A-39X-7, 15 cm) (XP). **4.** *Reticulofenestra hampdenensis* (Sample 189-1168A-44X-5, 120 cm) (XP). **5, 6.** *Reticulofenestra pseudoumbilicus* (Sample 189-1172A-21H-7, 15 cm); (5) Ph; (6) XP. **7.** *Reticulofenestra perplexa* (Sample 189-1170A-21X-2, 60 cm) (XP). **8.** *Reticulofenestra gelida* (Sample 189-1172A-10H-3, 117 cm) (XP). **9.** *Reticulofenestra minuta (*Sample 189-1168A-46X-1, 2 cm) (XP). **10, 11.** *Reticulofenestra haqii* (Sample 189-1172A-10H-3, 15 cm); (10) Ph; (11) XP. **12.** *Reticulofenestra producta* (Sample 189-1168A-11H-6, 15 cm) (XP).

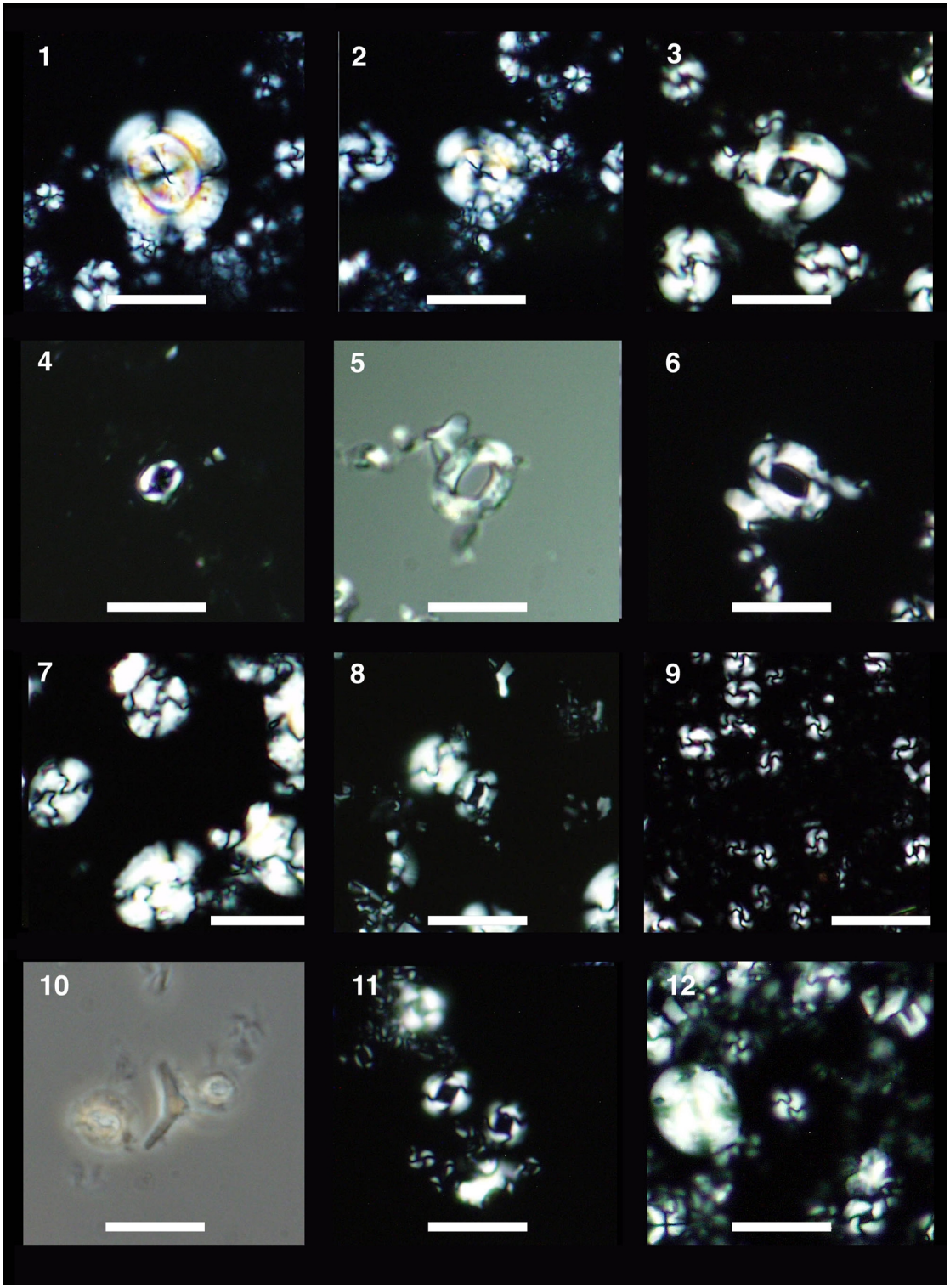

Plate P7. Scale bar = 10 µm. **1, 2.** *Triquetrorhabdulus carinatus* (Sample 189-1168A-45X-3, 61 cm); (1) differential-interference contrast light (DIC); (2) polarized light (XP). **3–6.** *Triquetrorhabdulus challengeri;* (3, 4) Sample 189-1168A-46X-2, 60 cm; (3) DIC; (4) XP; (5, 6) Sample 189-1168A-45X-3, 78 cm; (5) DIC; (6) XP. **7–10.** *Triquetrorhabdulus rugosus;* (7–9) Sample 189-1172A-14H-3, 15 cm; (7) phase-contrast light (Ph); (8) DIC; (9) XP; (10) Sample 189-1172A-12H-6, 15 cm (Ph). **11, 12.** *Triquetrorhabdulus farnsworthii* (Sample 189-1168A-24X-7, 15 cm); (11) Ph; (12) XP.

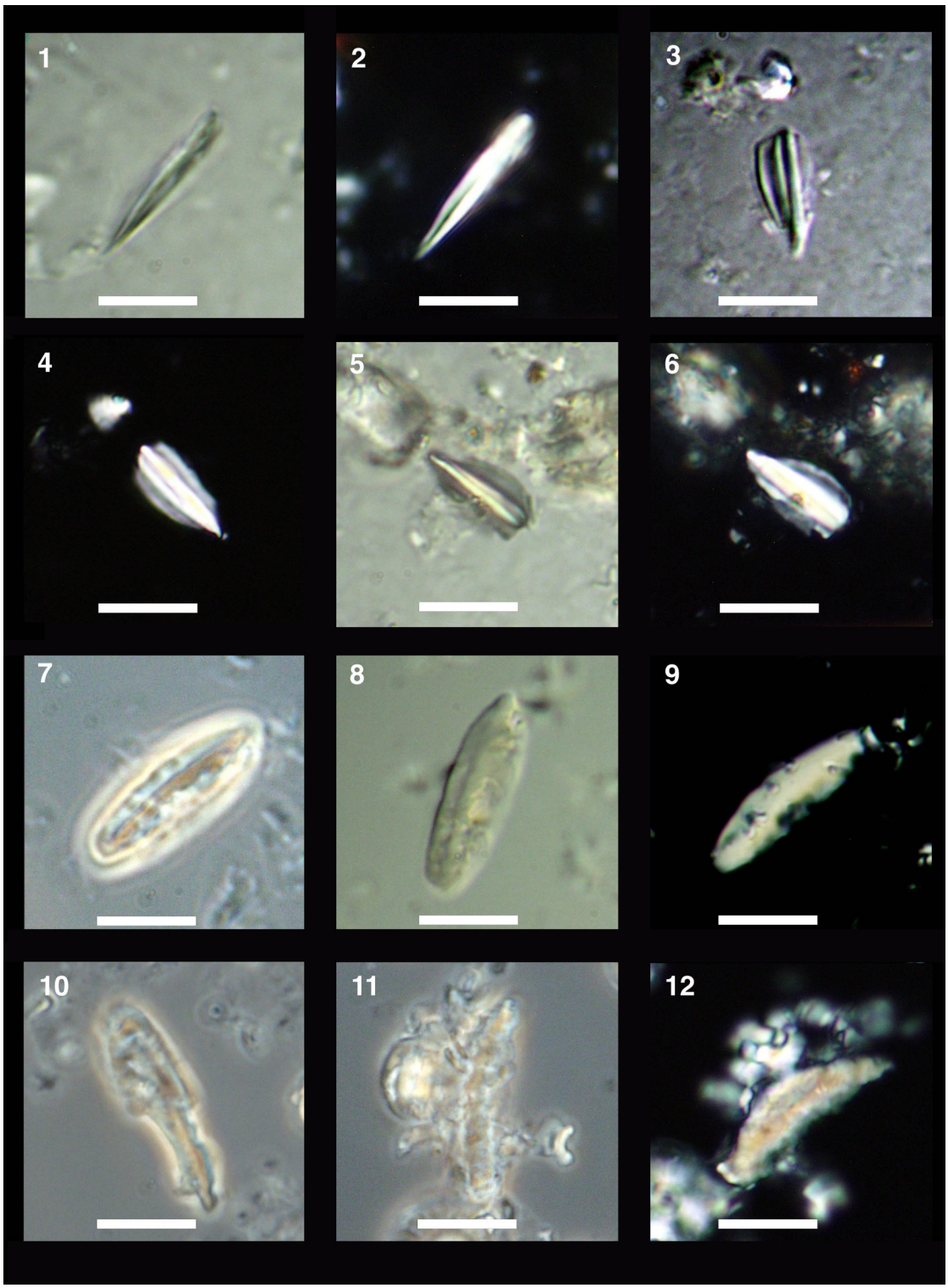

Plate P8. Scale bar = 10 µm. **1–3.** *Sphenolithus heteromorphus* (Sample 189-1172A-31X-4, 15 cm); (1) differential-interference contrast light (DIC); (2, 3) polarized light (XP). **4–7.** *Sphenolithus dissimilis* (Sample 189-1172A-35X-1, 18 cm); (4) phase-contrast light (Ph); (5) DIC; (6, 7) XP. **8–11.** *Sphenolithus disbelemnos* (Sample 189-1168A-33X-4, 15 cm); (8) Ph; (9) DIC; (10, 11) XP. **12.** *Sphenolithus capricornutus* (Sample 189-1168A-47X-2, 120 cm) (XP).

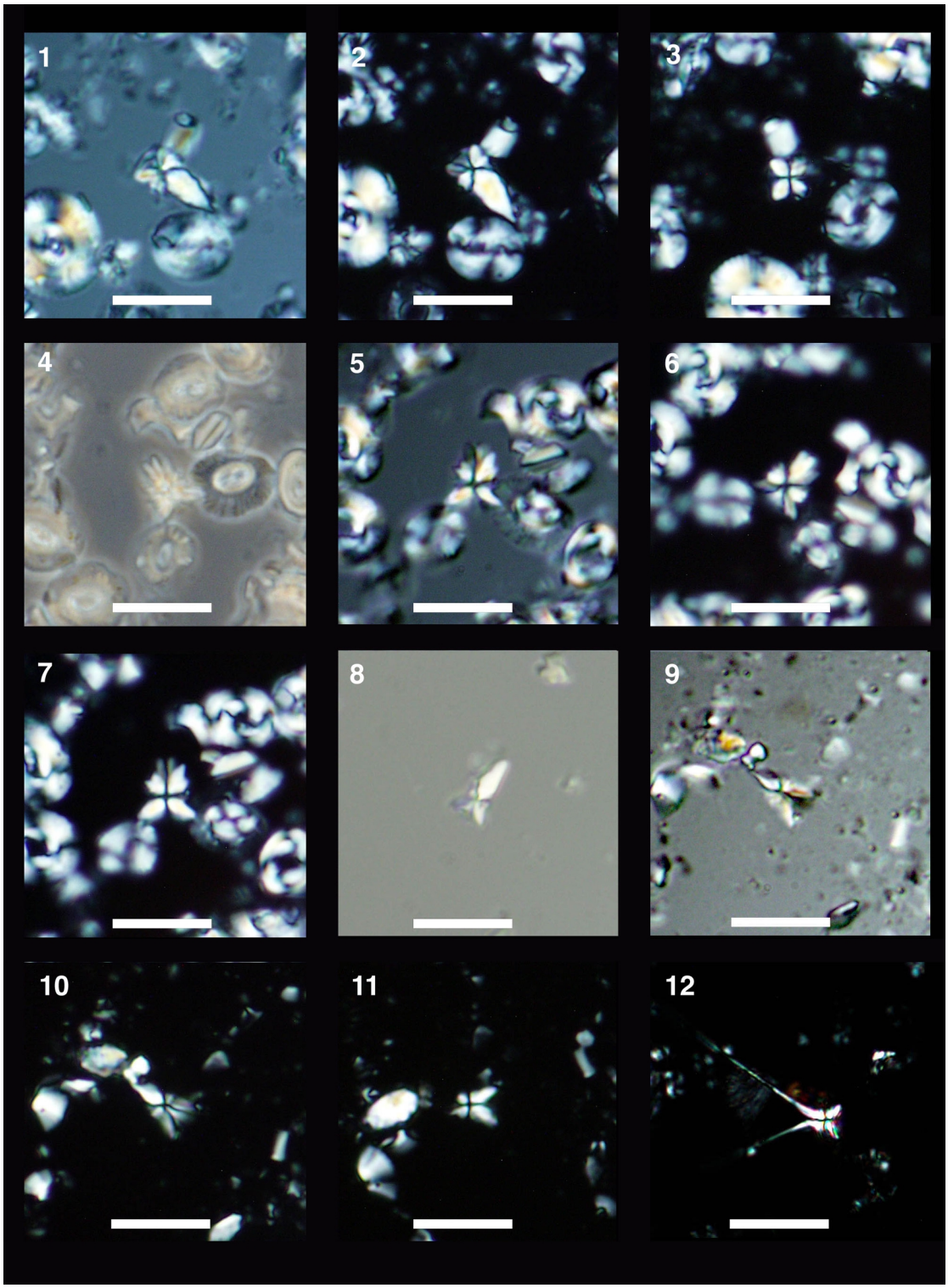

Plate P9. Scale bar = 10 µm. **1, 2.** *Coronocyclus nitescens* round (Sample 189-1170A-37X-1, 60 cm); (1) differential-interference contrast light (DIC); (2) polarized light (XP). **3, 4.** *Coronocyclus nitescens* oval (Sample 189-1171C-19X-6, 15 cm); (3) DIC; (4) XP. **5, 6.** *Sphenolithus moriformis* and *Sphenolithus conicus* (Sample 189-1168A-33X-4, 15 cm); (5) DIC; (6) XP. **7, 8.** *Scyphosphaera* sp. (Sample 189-1172A-11H-7, 15 cm); (7) phase-contrast light (Ph); (8) XP. **9, 10.** *Sphenolithus compactus* (Sample 189-1168A-44X-2, 120 cm); (9) DIC; (10) XP. **11, 12.** *Ilselithina fusa* (11) Sample 189-1168A-48X-2, 2 cm (XP); (12) Sample 189-1168A-46X-7, 2 cm (XP).

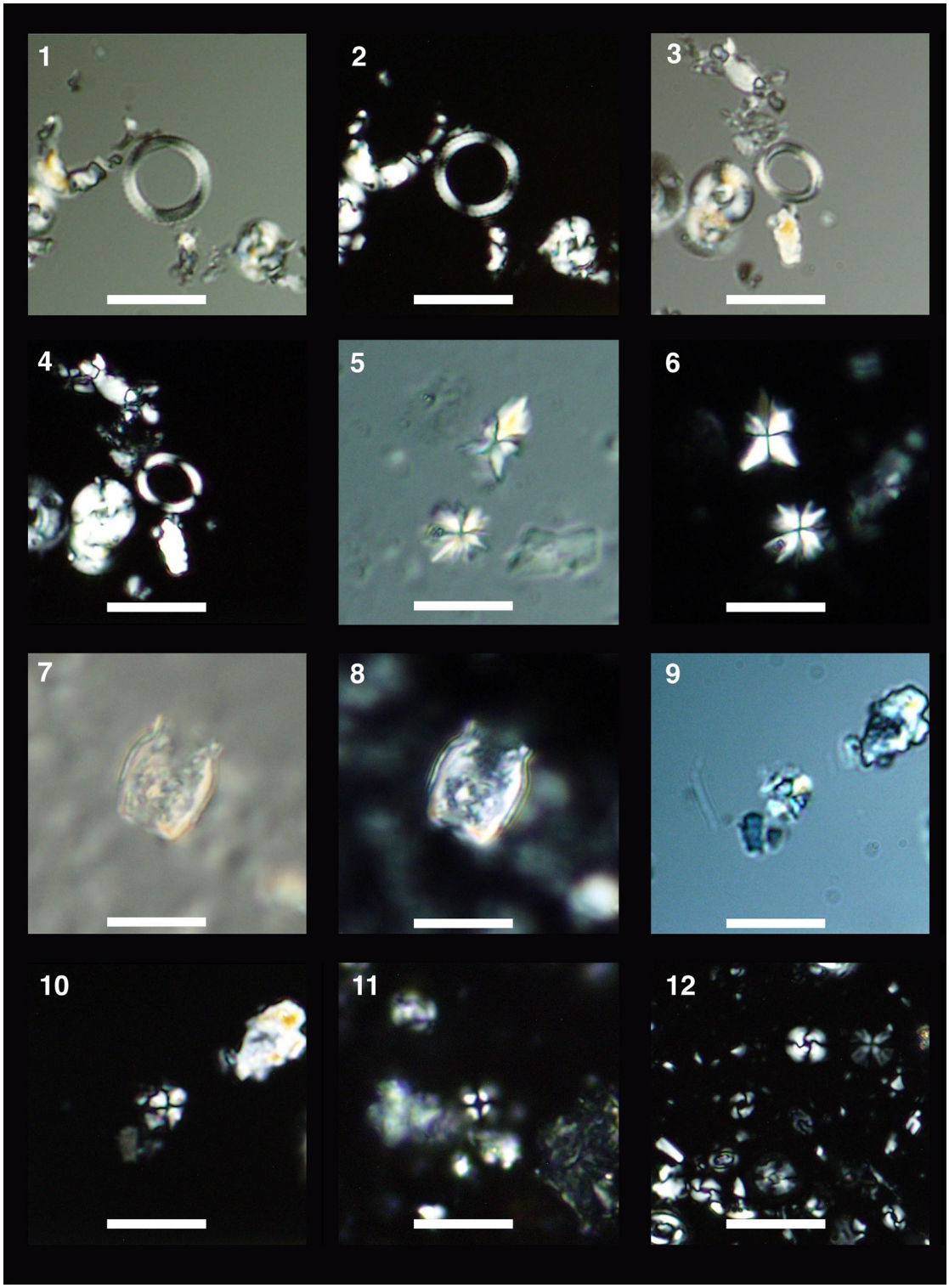

Plate P10. Scale bar = 10 µm. **1–3.** *Cryptococcolithus mediaperforatus* (Sample 189-1170A-23X-3, 60 cm); (1) phase-contrast light (Ph); (2) differential-interference contrast light (DIC); (3) polarized light (XP). **4–6.** *Umbilicosphaera jafari* (Sample 189-1168A-47X-2, 120 cm); (4) Ph; (5) DIC; (6) XP. **7–9.** *Pyrocyclus orangensis* (Sample 189-1168A-46X-7, 40 cm); (7) Ph; (8) DIC; (9) XP. **10.** *Pyrocyclus hermosus* (Sample 189-1172A-35X-1, 18 cm) (XP). **11, 12.** *Tetralithoides symeonidesii* (Sample 189-1168A-37X-5, 15 cm); (11) DIC; (12) XP.

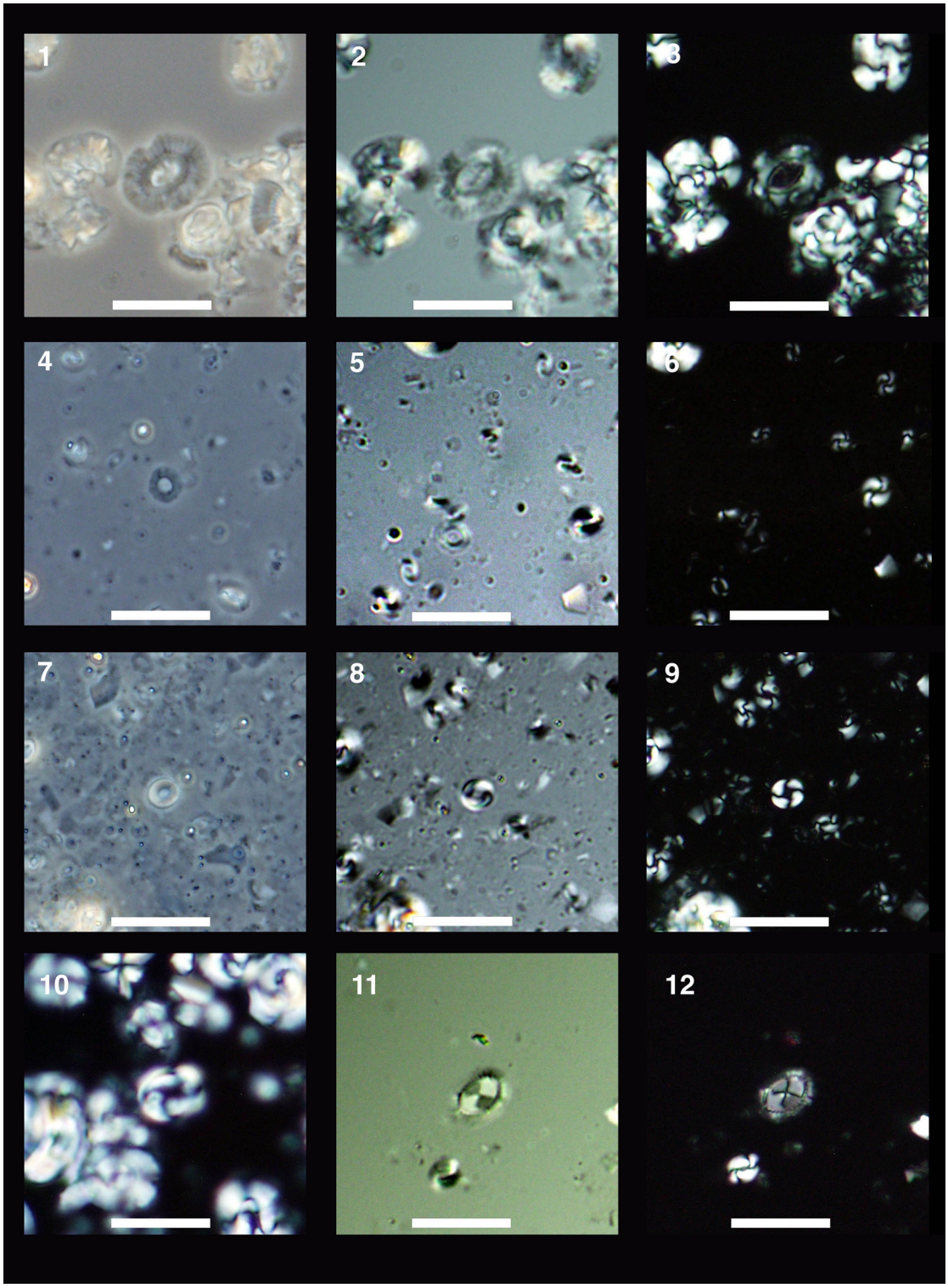

Plate P11. Scale bar = 10 µm. **1–3.** *Gemilithina rotula* (Sample 189-1170A-19X-3, 60 cm); (1) phase-contrast light (Ph); (2) differential-interference contrast light (DIC); (3) polarized light (XP). **4–6.** *Clausicoccus obrutus* (Sample 189-1168A-33X-1, 15 cm); (4) Ph; (5) DIC; (6) XP. **7, 8.** *Hughesius tasmaniae* (Sample 189-1168A-34X-5, 15 cm); (7) DIC; (8) XP. **9, 10.** *Camuralithus pelliculatus* (Sample 189-1168A-45X-2, 40 cm); (9) DIC; (10) XP. **11, 12.** *Ericsonia detecta* (Sample 189-1171C-22X-3, 15 cm); (11) Ph; (12) XP.

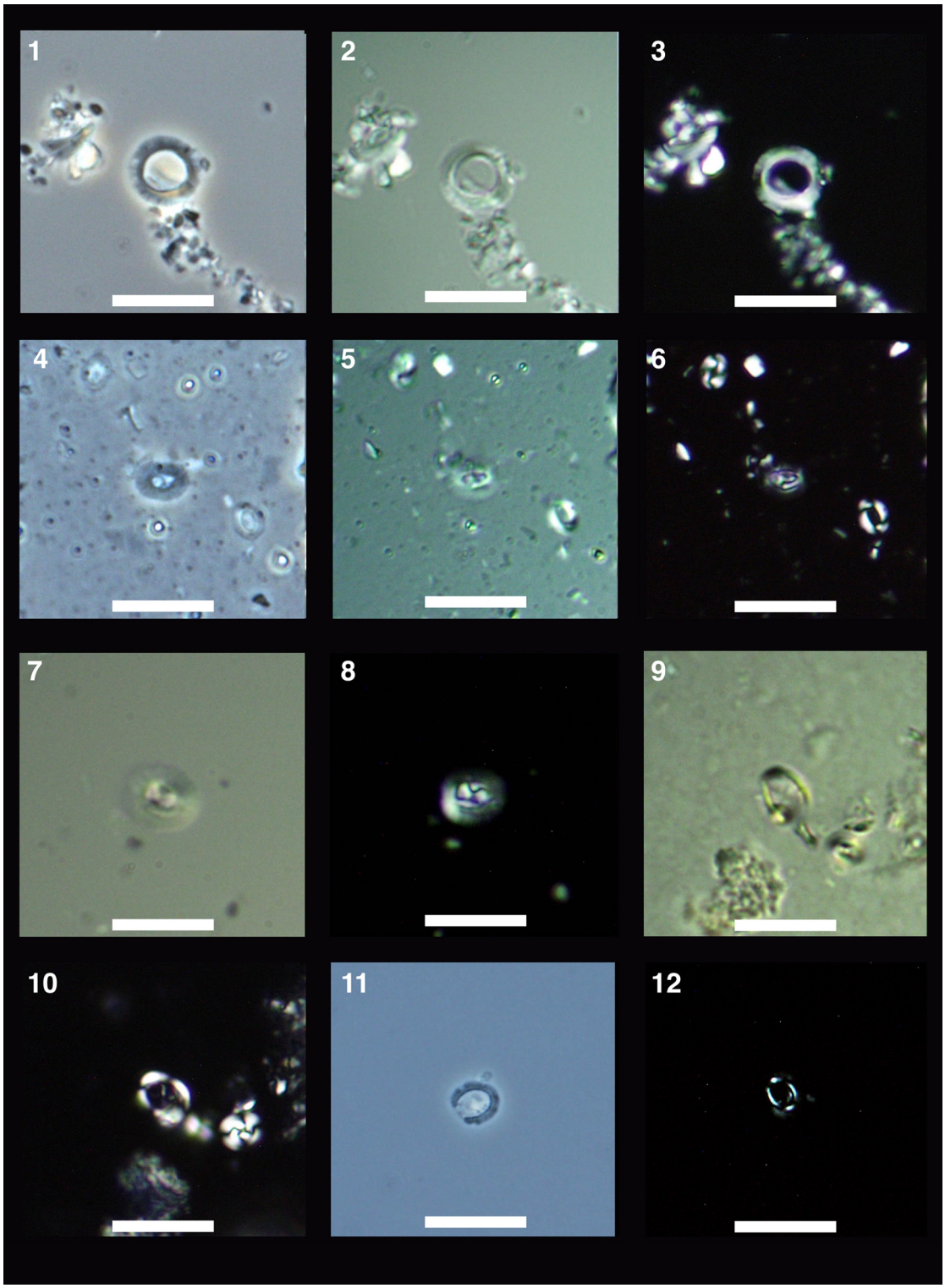

Plate P12. Scale bar = 10 µm. **1–3.** *Pontosphaera anisostrema* (Sample 189-1168A-47X-2, 120 cm); (1) phase-contrast light (Ph); (2) differential-interference contrast light (DIC); (3) polarized light (XP). **4–6.** *Pontosphaera multipora* (Sample 189-1168A-47X-2, 120 cm); (4) >12 µm (Ph); (5) DIC; (6) XP. **7.** *Pontosphaera desueta* (Sample 189-1168A-39X-4, 15 cm) (XP). **8.** *Coccolithus pelagicus* >12 µm (Sample 189-1171C-26X-1, 15 cm) (Ph). **9.** *Coccolithus miopelagicus* (Sample 189-1171C-25X-6, 15 cm) (Ph). **10–12.** *Minylitha convallis* (Sample 189-1168A-15X-2, 15 cm); (10) Ph; (11) DIC; (12) XP.

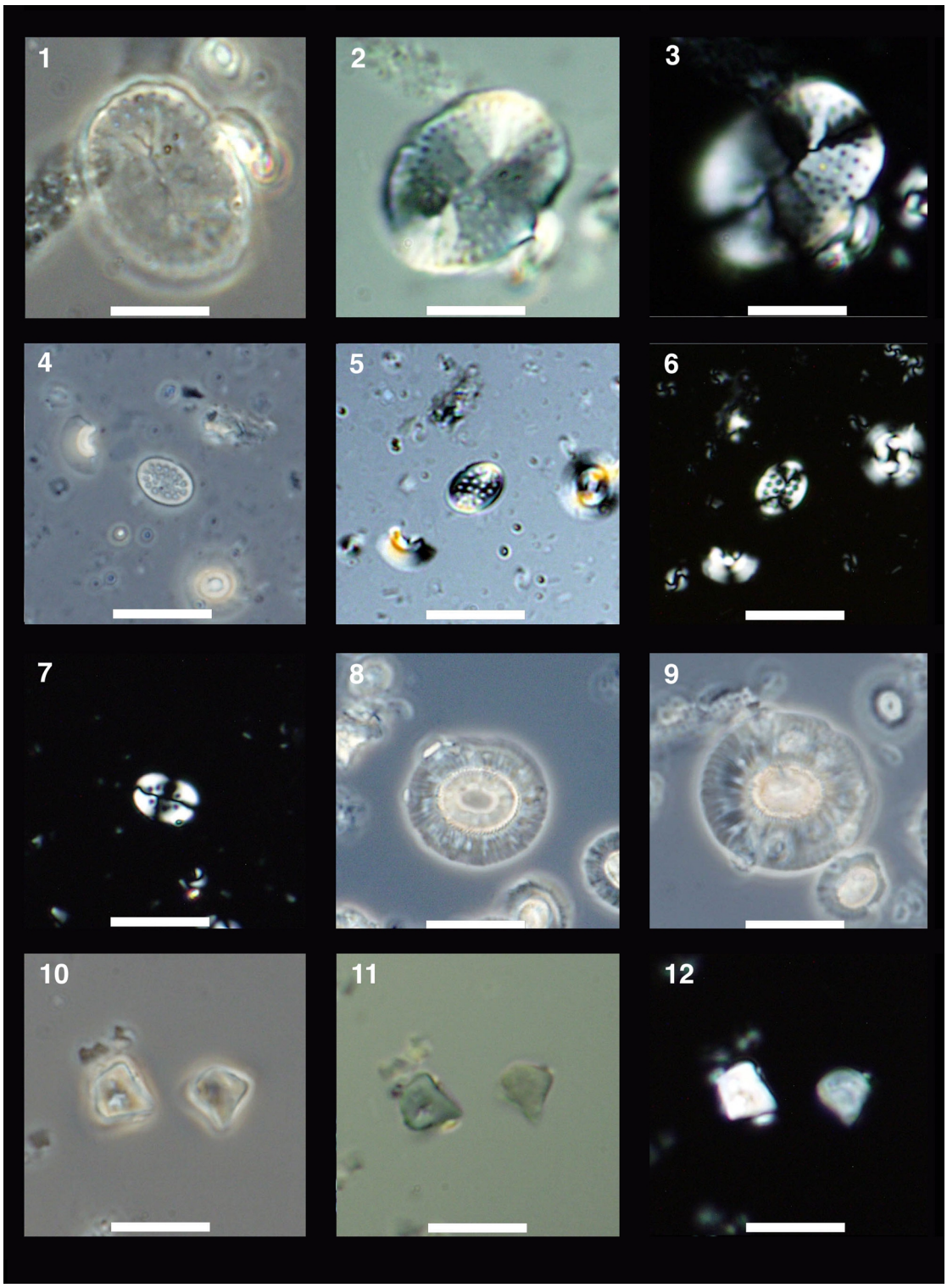

Plate P13. Scale bar = 10 µm. **1, 2.** *Reticulofenestra minutula* coccosphere (Sample 189-1172A-23H-3, 15 cm); (1) phase-contrast light (Ph); (2) polarized light (XP). **3, 6.** *Braarudosphaera bigelowii* (Sample 189-1168A-48X-1, 120 cm); (3) differential-interference contrast light (DIC); (6) XP. **4, 5.** *Reticulofenestra* sp. coccosphere (Sample 189-1171C-14X, 15 cm); (4) Ph; (5) XP. **7, 8.** *Calcidiscus leptoporus* coccosphere (Sample 189-1172A-14H-5, 15 cm); (7) DIC; (8) XP. **9, 12.** *Braarudosphaera discula* (Sample 189-1172A-31X-4, 15 cm); (9) DIC; (12) XP. **10.** *Rhabdosphaera procera* (Sample 189-1168A-47X-2, 120 cm) (Ph). **11.** *Sphenolithus compactus* (Sample 189-1172A-29X-2, 15 cm) (Ph).

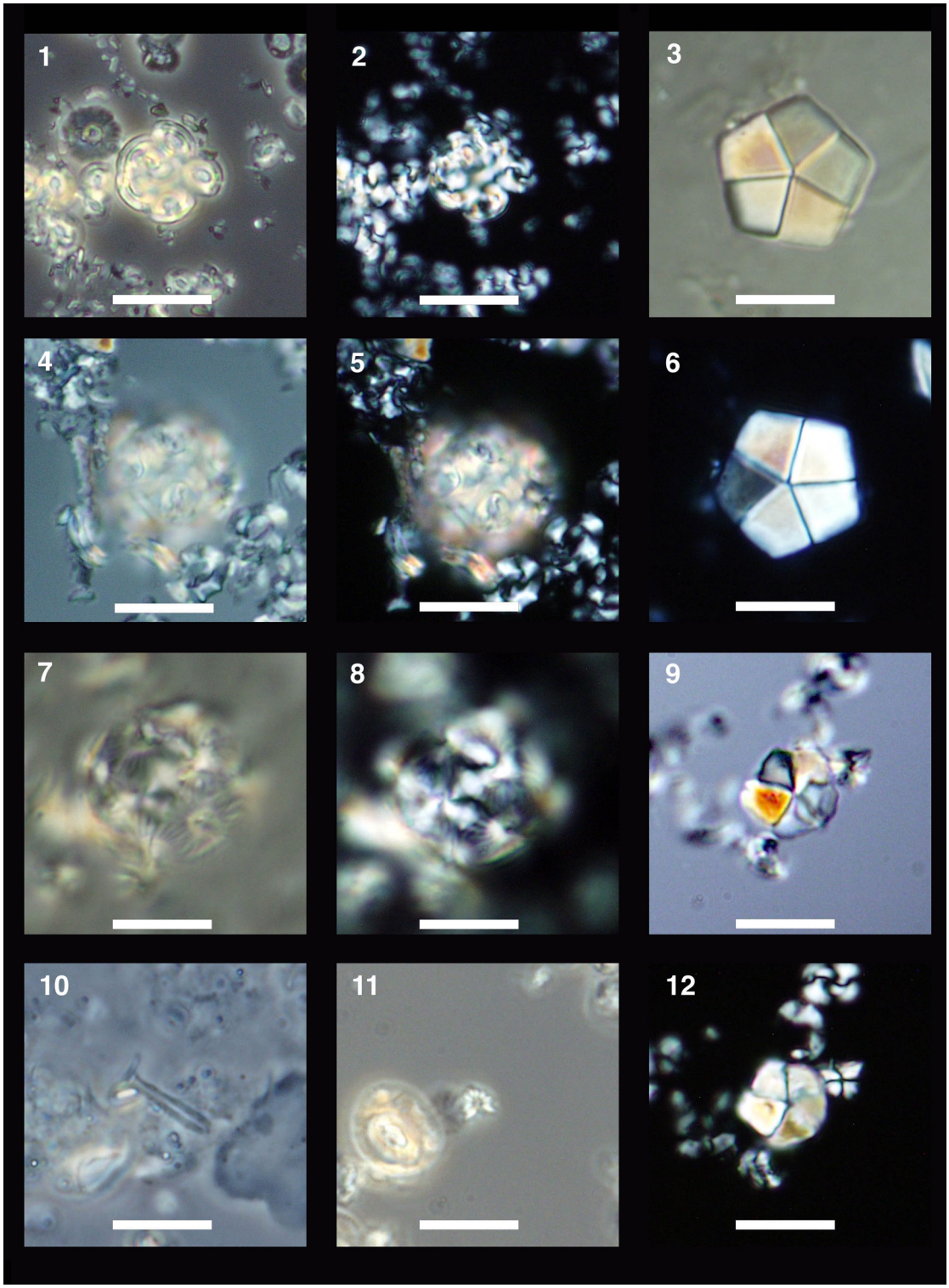

Appendix AT1. Calcareous nannofossils considered in this report (in alphabetic order of generic epithet). (Continued on next two pages.)

Species	Illustration	Reference	Notes
Amaurolithus amplificus		(Bukry and Percival, 1971) Gartner and Bukry, 1975	
Amaurolithus delicatus	**Pl. P2,** fig. 10	Gartner and Bukry, 1975	
Amaurolithus ninae	**Pl. P2,** fig. 11	(Bukry and Percival, 1971) Gartner and Bukry, 1975	
Amaurolithus primus	**Pl. P2,** fig. 9	(Bukry and Percival, 1971) Gartner and Bukry, 1975	
Amaurolithus tricorniculatus	**Pl. P2,** fig. 12	(Bukry and Percival, 1971) Gartner and Bukry, 1975	
Braarudosphaera bigelowii	**Pl. P13,** figs. 3, 6	(Gran and Braarud, 1935) Deflandre, 1947	
Braarudosphaera discula	**Pl. P13,** figs. 9, 12	Bramlette and Riedel, 1954	
Calcidiscus fuscus		(Backman, 1980) Janin 1987	
Calcidiscus kingii		(Roth, 1970) Loeblich and Tappan, 1978	
Calcidiscus leptoporus	**Pl. P5,** figs. 5, 6; **Pl. P13,** figs. 7, 8	(Murray and Blackman, 1898) Loeblich and Tappan, 1978	<11 µm, closed and open centers
Calcidiscus macintyrei	**Pl. P5,** figs. 10–12	(Bukry and Bramlette, 1966) Loeblich and Tappan, 1978	>11 µm, closed and open centers
Calcidiscus premacintyrei	**Pl. P5,** figs. 7–9	Theodoridis, 1984	>10 µm
Calcidiscus radiatus	**Pl. P5,** fig. 1	(Kamptner, 1954) Martin, Perez, and Aguodo, 1990	
Calcidiscus tropicus	**Pl. P5,** figs. 2–4	(Kamptner, 1954) Varol, 1989	
Camuralithus pelliculatus	**Pl. P11,** figs. 9, 10	de Kaenal and Villa, 1996	
Catinaster coalitus	**Pl. P1,** figs. 10–12	Martini and Bramlette, 1963	
Clausicoccus fenestratus		(Deflandre and Fert, 1954) Prins, 1979	
Clausicoccus obrutus	**Pl. P11,** figs. 4–6	(Perch-Nielsen, 1971) Prins, 1979	
Coccolithus miopelagicus	**Pl. P12,** fig. 9	(Bukry, 1971) Wise, 1973	>12 µm; central area <40% of total coccolith length (after Wise, 1973)
Coccolithus pelagicus		(Wallich, 1877) Schiller, 1930	
Coccolithus pelagicus >12 µm	**Pl. P12,** fig. 8		>12 µm
Coronocyclus aff. *prionion*		(Deflandre and Fert, 1954) Stradner in Stradner and Edward, 1968	
Coronocyclus nitescens	**Pl. P9,** figs. 1–4	(Kamptner, 1963) Bramlette and Wilcoxon, 1967	
Cryptococcolithus mediaperforatus	**Pl. P10,** figs. 1–3	(Varol, 1991) de Kaenel and Villa, 1996	
Cyclicargolithus abisectus		(Müller, 1970) Wise, 1973	>11 µm
Cyclicargolithus floridanus	**Pl. P3,** figs. 10–12	(Hay et al., 1967) Bukry, 1971	
Discoaster asymmetricus		Gartner, 1969	
Discoaster bellus	**Pl. P1,** fig. 1	Bukry and Percival, 1971	
Discoaster berggrenii	**Pl. P2,** fig. 8	Bukry, 1971	
Discoaster bollii		Martini and Bramlette, 1963	
Discoaster braarudii	**Pl. P1,** fig. 7	Bukry, 1971	
Discoaster brouweri		(Tan, 1927) Bramlette and Riedel, 1954	
Discoaster challengeri	**Pl. P1,** fig. 4	Bramlette and Riedel, 1954	
Discoaster deflandrei	**Pl. P1,** fig. 8	Bramlette and Riedel, 1954	
Discoaster exilis	**Pl. P1,** fig. 5	Martini and Bramlette, 1963	
Discoaster extensus	**Pl. P1,** fig. 6.		
Discoaster hamatus	**Pl. P2,** fig. 5	Martini and Bramlette, 1963	
Discoaster intercalaris		Bukry, 1971	
Discoaster loeblichii	**Pl. P2,** fig. 1	Bukry, 1971	
Discoaster mendomobensis		Wise, 1973	
Discoaster pentaradiatus		(Tan, 1927) Bramlette and Riedel, 1954	
Discoaster petaliformis		Moshkovitz and Ehrlich, 1980	
Discoaster quinqueramus	**Pl. P2,** figs. 6, 7	Gartner, 1969	
Discoaster spp. (5 ray)	**Pl. P1,** figs. 2, 3		
Discoaster spp. (6 ray)	**Pl. P1,** fig. 9		
Discoaster surculus	**Pl. P2,** figs. 2, 3	Martini and Bramlette, 1963	
Discoaster triradiatus	**Pl. P2,** fig. 4	Tan, 1927	
Discoaster variabilis		Martini and Bramlette, 1963	
Ericsonia detecta	**Pl. P11,** figs. 11, 12	de Kaenal and Villa, 1996	

Appendix AT1 (continued).

Species	Illustration	Reference	Notes
Geminilithella rotula	**Pl. P11,** figs. 1–3	(Kamptner, 1956) Backman, 1980	
Hayaster perplexus		(Bramlette and Riedel, 1954), Bukry, 1973	
Helicosphaera ampliaperta	**Pl. P3,** figs. 1–4	Bramlette and Wilcoxon, 1967	
Helicosphaera bramlettei		(Müller, 1970) Jafar and Martini, 1975	
Helicosphaera carteri		(Wallich, 1877) Kamptner, 1954	
Helicosphaera compacta	**Pl. P4,** figs. 4–7	Bramlette and Wilcoxon, 1967	
Helicosphaera elongata	**Pl. P3,** figs. 8, 9	Theodoridis, 1984	
Helicosphaera euphratis	**Pl. P3,** figs. 10–12	Haq, 1966	
Helicosphaera granulata		(Bukry and Percival, 1971) Jafar and Martini, 1975	
Helicosphaera mediterranea		Müller, 1981	
Helicosphaera obliqua	**Pl. P4,** figs. 8–10	Bramlette and Wilcoxon, 1967	
Helicosphaera orientalis		Bukry, 1971	
Helicosphaera paleocarteri	**Pl. P3,** figs. 10–12; **Pl. P4,** figs. 1–3	Theodoridis, 1984	
Helicosphaera perch-nielsenae	**Pl. P4,** figs. 11, 12	(Haq, 1971) Jafar and Martini, 1975	
Helicosphaera recta	**Pl. P3,** figs. 5–7	(Haq, 1966) Jafar and Martini, 1975	
Helicosphaera scissura		Miller, 1981	
Helicosphaera sellii		(Bukry and Bramlette, 1969) Jafar and Martini, 1975	
Helicosphaera spp.			
Helicosphaera wilcoxonii		(Gartner, 1971) Jafar and Martini, 1975	
Hughesius gizoensis		Varol, 1989	
Hughesius tasmaniae	**Pl. P11,** figs. 7, 8	(Edward and Perch-Nielsen, 1975) de Kaenel and Villa, 1996	
Ilselithina fusa	**Pl. P9,** figs. 11, 12	Roth, 1970	
Minylitha convallis	**Pl. P12,** figs. 10–12	Bukry, 1973	
Pontosphaera anisotrema	**Pl. P12,** figs. 1–3	(Kamptner, 1956) Backman, 1980	
Pontosphaera desueta	**Pl. P12,** fig. 7	(Müller, 1970) Perch-Nielsen, 1984	
Pontosphaera multipora	**Pl. P12,** figs. 4–6	(Kamptner, 1948) Burns, 1973	
Pontosphaera spp.			
Pyrocyclus hermosus	**Pl. P10,** fig. 10	Roth and Hay in Hay et al., 1967	
Pyrocyclus orangensis	**Pl. P10,** figs. 7–9	(Bukry, 1971) Backman, 1980	
Reticulofenestra bisecta bisecta	**Pl. P6,** fig. 2	(Hay, Mohler, and Wade, 1966) Roth, 1970	<10 µm
Reticulofenestra bisecta filewiczii		(Hay, Mohler, and Wade, 1966) Roth, 1970 filewiczii Wise and Wiegand in Wise, 1983	Small central plate
Reticulofenestra coenura		(Reinhardt, 1966) Roth, 1970	
Reticulofenestra gelida	**Pl. P6,** fig. 8	(Geitzenauer, 1972) Backman, 1978	>7 µm; small central opening
Reticulofenestra hampdenensis	**Pl. P6,** fig. 4	Edwards, 1973	
Reticulofenestra haqii	**Pl. P6,** figs. 10, 11	Backman, 1978	3–5 µm; central opening > 1.5 µm
Reticulofenestra lockeri	**Pl. P6,** fig. 3	Müller, 1970	
Reticulofenestra minuta	**Pl. P6,** fig. 9	Roth, 1970	1.5–2 µm in length
Reticulofenestra minutula	**Pl. P13,** figs. 1, 2	(Gartner, 1967) Haq and Berggren, 1978	3–5 µm; central opening < 1.5 µm
Reticulofenestra perplexa	**Pl. P6,** fig. 7	(Burns, 1975) Wise, 1983	6–9 µm
Reticulofenestra producta	**Pl. P6,** fig. 12	(Kamptner, 1963) Wei and Thierstein, 1991	3–4 µm
Reticulofenestra pseudoumbilicus	**Pl. P6,** figs. 5, 6	(Gartner, 1967) Gartner, 1969	>7 µm; large central opening
Reticulofenestra stavensis	**Pl. P6,** fig. 1	(Levin and Joerer, 1967) Varol, 1989	
Rhabdosphaera gladius		Locker, 1967	
Rhabdosphaera procera	**Pl. P13,** fig. 10	(Martini, 1969) Jafar, 1975	
Sphenolithus abies		Deflandre in Deflandre and Fert, 1954	
Sphenolithus belemnos		Bramlette and Wilcoxon, 1967	
Sphenolithus calyculus		Bukry, 1985	
Sphenolithus capricornutus	**Pl. P8,** fig. 12	Bukry and Percival, 1971	
Sphenolithus ciperoensis		Bramlette and Wilcoxon, 1967	
Sphenolithus cometa		de Kaenal and Villa, 1996	

Appendix AT1 (continued).

Species	Illustration	Reference	Notes
Sphenolithus compactus	**Pl. P9,** figs. 9, 10; **Pl. P13,** fig. 11	Backman, 1980	
Sphenolithus conicus	**Pl. P9,** figs. 5, 6	Bukry, 1971	
Sphenolithus delphix		Bukry, 1973	
Sphenolithus disbelemnos	**Pl. P8,** figs. 8–11	Fornaciari and Rio, 1996	
Sphenolithus dissimilis	**Pl. P8,** figs. 4–7	Bukry and Percival, 1971	
Sphenolithus grandis		Haq and Berggren, 1978	
Sphenolithus heteromorphus	**Pl. P8,** figs. 1–3	Deflandre, 1953	
Sphenolithus moriformis	**Pl. P8,** figs. 5, 6	(Brönnimann and Stradner, 1960) Bramlette and Wilcoxon, 1967	
Sphenolithus moriformis <6 µm			<6 µm
Sphenolithus neoabies		Bukry and Bramlette, 1969	
Sphenolithus spp.			
Sphenolithus verensis		Backman, 1978	
Scyphosphaera spp.	**Pl. P9,** figs. 7, 8		
Tetralithoides sygmeonidesii	**Pl. P10,** figs. 11, 12	Theodoridis, 1984	
Triquetrorhabdulus auritus		Stradner and Allram, 1982	
Triquetrorhabdulus carinatus	**Pl. P7,** figs. 1, 2	Martini, 1965	
Triquetrorhabdulus challengeri	**Pl. P7,** figs. 3–6	Perch-Nielsen, 1977	
Triquetrorhabdulus farnsworthii	**Pl. P7,** figs. 11, 12	(Gartner, 1967) Perch-Nielsen, 1984	
Triquetrorhabdulus milowii		Bukry, 1971	
Triquetrorhabdulus rugosus	**Pl. P7,** figs. 7–10	Bramlette and Wilcoxon, 1967	
Umbilicosphaera jafari	**Pl. P10,** figs. 4–6	Müller, 1974	
Umbilicosphaera spp.			
Zygrhablithus bijugatus		(Deflandre in Deflandre and Fert, 1954) Deflandre, 1959	